Mesoscopic hydrothermodynamics of complex-structured materials

Áurea R. Vasconcellos,[1,*] A. A. P. Silva,[2] Roberto Luzzi,[1,†] J. Casas-Vázquez,[3] and David Jou[3,4]
[1]*Condensed Matter Physics Department, Institute of Physics "Gleb Wataghin," University of Campinas, Unicamp. 13083-859 Campinas, SP, Brazil*
[2]*Departamento de Ciências Exatas, Universidade Federal de Lavras, UFLA. 37200-000 Lavras, MG, Brazil*
[3]*Departament de Física, Universitat Autónoma de Barcelona, 08193 Bellaterra, Catalunya, Spain*
[4]*Institut d'Estudis Catalans, Carme 47, 08001 Barcelona, Catalunya, Spain*
(Received 12 December 2011; published 7 October 2013)

Some experimental results in the study of disordered systems, polymeric fluids, solutions of micelles and surfactants, ionic-glass conductors, and others show a hydrodynamic behavior labeled "anomalous" with properties described by some kind of fractional power laws in place of the standard ones. This is a consequence of the fractal-like structure that is present in these systems of which we do not have a detailed description, thus impairing the application of the conventional ensemble formalism of statistical mechanics. In order to obtain a physical picture of the phenomenon for making predictions which may help with technological and industrial decisions, one may resort to different styles (so-called nonconventional) in statistical mechanics. In that way can be introduced a theory for handling such impaired situations, a nonconventional mesoscopic hydrothermodynamics (MHT). We illustrate the question presenting an application in a contracted description of such nonconventional MHT, consisting in the use of the Renyi approach to derive a set of coupled nonstandard evolution equations, one for the density, a nonconventional Maxwell-Cattaneo equation, which in a limiting case goes over a non-Fickian diffusion equation, and other for the velocity in fluids under forced flow. For illustration the theory is applied to the study of the hydrodynamic motion in several soft-matter systems under several conditions such as streaming flow appearing in electrophoretic techniques and flow generated by harmonic forces arising in optical traps. The equivalence with Lévy processes is discussed and comparison with experiment is done.

DOI: 10.1103/PhysRevE.88.042110 PACS number(s): 05.70.−a, 47.57.J−, 66.10.C−, 05.40.Fb

I. INTRODUCTION

The question of a so-called nonstandard hydrodynamics is associated with disordered media [1], consisting in that disordered systems do not follow the classical laws which describe transport in ordered systems and that this leads to many kinds of unexpected physical properties that differ from the ones of standard hydrodynamics. The range of applicability and of physical interest is enormous, as, for instance, colloidal particles, surfactant micelles, and polymer solutions, which are classical examples of what is soft-condensed matter [2]. One particular case is the so-called non-Fickian diffusion described by a time evolution following a kind of fractional power law [3]. This seems to be connected with the fact that the motion is proceeding in a medium with a fractal-like structure [4]. This is of relevance in technological areas, as it is the case of luminescence in quantum wells with fractal-like boundaries in semiconductor heterostructures [5] and "anomalous" results in cyclic voltammetry experiments involving fractal electrodes in microbatteries which can be interpreted in terms of non-Fickian diffusion of charges in the electrolyte [6].

Of particular relevance is the application of polymers in electronics and photonics [7–14]. These materials display a wide variety of unusual rheological phenomena, which are of great importance to the synthesis, processing, and end-use characteristics of them [15,16]. For instance, the diffusion behavior of the so-called glassy polymers or of micelles exhibits "non-Fickian" behavior [3]. In those cases, the question of how flow (advective motion, particularly under shear flow [17]) affects the system, a vital topic in many situations, including the production of food, derivatives of petroleum, and household goods, and in various applications in medicine, has come forth. Particularly, the prediction of the flow of complex fluids, such as solutions of surfactants or polymers, through porous media is of particular interest to various industrial processes, e.g., many oil industry treatments, when modeling based on macroscopic approximations tends to fail [18]. We present in this paper a study of the motion of a fluid in the presence of a forced flow (advective motion) in the framework of what can be called a nonconventional hydrothermodynamics based on microscopic basis, that is, a mechanical-statistical approach built in terms of a nonconventional nonequilibrium statistical ensemble formalism [19]. This implies the introduction of a particular kind of unification of kinetic and hydrodynamic approaches adapted for dealing with complex structured systems. In other words, we propose here a *reformulation of mesoscopic hydrothermodynamics* [20–22] *in terms of such a nonconventional nonequilibrium statistical ensemble formalism (NCNESEF)*.

Thus, in the case of these systems showing fractal-like structural characteristics, the treatment is outside the domain of classical hydrodynamics, as we discuss below, and a proper handling of the problem is quite difficult, if not inaccessible. A way to obtain some kind of prediction on the behavior of the system can be done resorting to NCNESEF, which thus enters into play when the standard ensemble approach to the well-established logically and physically sound Boltzmann-Gibbs statistics cannot be properly applied, as one does not possess an access to the relevant and proper characterization of the

[*]Deceased October 13, 2012.
[†]http://www.ifi.unicamp.br/∼aurea

system in the given experimental conditions. This signifies that one is facing the question of existence of the so-called hidden constraints. There exists a large family of these statistics, as shown in Ref. [23], and in the case of the hydrodynamic motion in complex-structured fluids as those we have mentioned, it can be used Renyi's approach [24,25], whose application and validity in physics have been summarized and discussed in the work by Jizba and Arimitsu in Ref. [26].

It should be stressed that a complete physical picture of the phenomenon has not been obtained; however, it is possible to make predictions obtaining a relatively clear interpretation of the facts involved in the physical processes. The use of the theory is illustrated through its application to the study of surfactant micelles and polymer solutions. Also, it is shown that, for this particular case, there is an equivalence of results with those obtained in a description in terms of Lévy modified normal distribution (see Sec. IV). Additional considerations are presented under Discussion and Concluding Remarks. In Sec. V we discuss application of the theory to non-Fickian diffusion in soft matter and where the analysis of specific experiments is done.

II. HYDRODYNAMIC MOTION IN COMPLEX-STRUCTURED FLUIDS

As already presented in the Introduction, in some systems there occurs a kind of unexpected hydrodynamic motion [1–3,27–29] in the sense that the standard hydrodynamic equations do not properly describe the experimental results, which show some type of power law that differs from the usual one.

This is the case of polymer solutions where, as a consequence, there are present macromolecules differing in chain structure and mass, implying in the coupling of the translational motion with the vibrational and rotational ones [30–32], which strongly influences the motion, that cannot be properly described in terms of the movement of the center of mass alone. It can be expected to find a variety of structures in the medium with a certain space distribution of a fractal-like character.

It is worth noticing that something similar is present in art (in Jackson Pollock paintings) [33]. Because of this, the usual classical (Onsagerian) hydrothermodynamics (leading to, for example, Fick and Fourier transport laws) is not properly applicable. Moreover, density-density and velocity-velocity correlations may be relevant if entanglement of macromolecules is not negligible and nonlinearities are at work which can produce complex behavior and hydrodynamic instabilities [34].

As noted before in, for example, polymer solutions, the macromolecules differ in mass and in configuration, which greatly influences the movement, which would be the result of a certain distribution of masses and including, besides the translational movement, the influence of the internal degrees of freedom and their coupling with the translational one, as well as the effects of dangling, entanglement, breaking, and recombination, so we are facing the question of the presence of the already-mentioned "hidden constraints." To face situations of this kind, one may resort to the use of the auxiliary statistics developed for dealing with the existence of hidden constraints. For a general view, see Ref. [23], and in the context of physics we shall refer to them as NCNESEF [19].

Nonconventional statistical mechanics is described elsewhere (see Refs. [19] and [35]) and here we simply notice that NCNESEF consists of two steps: (1) The choice of a *heterotypical probability distribution* (derived in a variational method from a heterotypical quantity of uncertainty of information, also called informational entropy, of which there are a large number of alternatives [19]) and (2) the use in the calculation of average values of the so-called *escort probability* [19,23,35,36], written in terms of the former [see Eq. (11) below]. Through item (2) are introduced correlations (fluctuations and higher-order variances) of the basic quantities, and through item (1) are introduced modified populations of the states of the system; we return to these points at the end of the section.

For dealing with the hydrodynamic motion in complex-structured fluids, which involves, as noted, the observation of unexpected behavior, we resort here to a derivation of the hydrodynamic equations at the kinetic level but in the framework of a NCNESEF, and, particularly, we use the one based on the Renyi approach. The latter is by far the most accepted and a quite effective one (Refs. [23,25,26]).

The so-called mesoscopic hydrothermodynamics (or nonlinear higher-order hydrodynamics) in the framework of a nonequilibrium statistical ensemble formalism (NESEF) consists of a description in terms of the densities of energy and matter and their fluxes of all orders, together with their direct and cross-correlations. MHT follows from the application of the moments method to the solution of the kinetic equation for the single-particle distribution function, $f_1(\mathbf{r},\mathbf{p};t)$, at the classical-mechanics level [21,22].

Such moments (in $\mathbf{p}$ space) are the hydrodynamic variables

$$n(\mathbf{r},t) = \int d^3p\, f_1(\mathbf{r},\mathbf{p};t), \tag{1}$$

the density of particles,

$$\mathbf{I}_n(\mathbf{r},t) = \int d^3p\, \frac{\mathbf{p}}{m}\, f_1(\mathbf{r},\mathbf{p};t), \tag{2}$$

the first flux of n (multiplied by m is the linear momentum density),

$$I_n^{[l]}(\mathbf{r},t) = \int d^3p\, u^{[l]}(\mathbf{p})\, f_1(\mathbf{r},\mathbf{p};t), \tag{3}$$

with $l = 1,2,3\ldots$ the higher-order fluxes of n,

$$u^{[l]}(\mathbf{p}) = \left[\frac{\mathbf{p}}{m}\ldots(l)\times\ldots\frac{\mathbf{p}}{m}\right], \tag{4}$$

i.e., the tensor of l rank resulting of the tensorial inner product of l vectors $\frac{\mathbf{p}}{m}$ (the group velocity of the particle).

Similarly, for the density of kinetic energy,

$$h(\mathbf{r},t) = \int d^3p\, \frac{p^2}{2m}\, f_1(\mathbf{r},\mathbf{p};t), \tag{5}$$

$$I_h^{[l]}(\mathbf{r},t) = \int d^3p\, \frac{p^2}{2m}\, u^{[l]}(\mathbf{p})\, f_1(\mathbf{r},\mathbf{p};t), \tag{6}$$

with $l = 1,2,3\ldots$.

The hydrodynamic equations are

$$\frac{\partial}{\partial t} I_n^{[l]}(\mathbf{r},t) = \int d^3p\, u^{[l]}(\mathbf{p})\, \frac{\partial}{\partial t} f_1(\mathbf{r},\mathbf{p};t), \tag{7}$$

and similarly for the energy "family." They are given in Ref. [21]; at the quantum-mechanical level they are given in Refs. [38,39].

This set of hydrodynamic equations derived from Eq. (7) [21] is practically intractable and then one is forced to resort to drastically reduce the set of basic variables to a small one, that is, disregard higher-order fluxes—usually larger than the second one, which die down in very short time intervals. In other words, one must—for each case—*retain the information considered as relevant for the problem at hand and disregard nonrelevant information*. We have discussed the reduction of the dimensions of the nonequilibrium thermodynamic space of states elsewhere [37]. A criterion for justifying the different levels of contraction is derived: It depends on the range of wavelengths and frequencies which are relevant for the characterization, in terms of normal modes, of the hydrothermodynamic motion in the nonequilibrium open system. The Maxwell times, associated to the different fluxes, have a particular relevance for deciding the order of the contraction of description [37].

The kinetic equation or generalized Boltzmann equation for $f_1(\mathbf{r},\mathbf{p};t)$, the classical one, is given in Ref. [22], and the quantum one (generalized Boltzmann-Wigner-von Neumann equation) in Refs. [38,39], all in the conventional standard situation. Nonconventional mesoscopic hydrothermodynamics (NCMHT) follows from the use of a nonconventional single-particle distribution function, as the one presented in Appendix A given in so-called Renyi statistics.

Next we illustrate the matter considering a particular contracted description (a MHT of order 1) in which we keep only the variables,

$$\{h(\mathbf{r},t),\, n(\mathbf{r},t),\, \mathbf{I}_n(\mathbf{r},t)\}, \tag{8}$$

that is, the energy density, the density of particles, and the first-order flux (current). (The criteria for establishing the order of the truncation is considered in Ref. [37].)

Let us proceed to derive the evolution equations of the basic quantities in set (8) using Renyi's approach to nonconventional statistics. In that way we are led to obtain non-conventional hydrodynamic equations which are accompanied with an adjustable power index, which, as noted in the Introduction, depends on the dynamics, fractality, geometry and dimensions, the thermodynamic state of the system, and the experimental protocol (several examples are presented in Ref. [19]). The first-order description, characterized by the variables in set (8), disregards shear stress, which can be incorporated using a second-order hydrothermodynamics, that is, to include in the basic set the second-order flux, $I_n^{[2]}(\mathbf{r},t)$, which is proportional to the pressure tensor [21,22]. To obtain the hydrodynamic equations, we first proceed to separate the Hamiltonian into two contributions, namely

$$\hat{H} = \hat{H}_0 + \hat{H}', \tag{9}$$

where $\hat{H}_0$ is the kinetic energy and $\hat{H}'$ contains all the interactions that are present in the system, including the action of external forces and interactions with reservoirs. Moreover, in a classical approach, the basic microdynamic variables, corresponding to the macroscopic variables in set (8), are

$$\hat{h}(\mathbf{r}|\Gamma) = \int d^3\mathbf{p} \left(\frac{p^2}{2m}\right) \hat{n}_1(\mathbf{r},\mathbf{p}|\Gamma), \tag{10}$$

$$\hat{n}(\mathbf{r}|\Gamma) = \int d^3\mathbf{p}\ \hat{n}_1(\mathbf{r},\mathbf{p}|\Gamma), \tag{11}$$

$$\hat{\mathbf{I}}_n(\mathbf{r}|\Gamma) = \int d^3\mathbf{p} \left(\frac{\mathbf{p}}{m}\right) \hat{n}_1(\mathbf{r},\mathbf{p}|\Gamma), \tag{12}$$

where m is the mass of the particles, $\mathbf{p}$ the linear momentum, and $\hat{n}_1$ the reduced single-particle density function,

$$\hat{n}_1(\mathbf{r},\mathbf{p}|\Gamma) = \sum_{j=1}^{N} \delta(\mathbf{r}-\mathbf{r}_j)\delta(\mathbf{p}-\mathbf{p}_j), \tag{13}$$

with N being the number of particles and Γ a point in phase space. Equation (10) corresponds to the density of kinetic energy: for simplicity of description of the formalism, and because that is the situation in dilute solutions to be studied in following sections, interaction between the particles is not included. The dynamical quantities of Eqs. (10) to (12) provide, in this contracted description, the basis for the kinetic approach to hydrodynamics in the NESEF framework [22,35,38], which, for the complex structured materials that present hidden constraints that we consider here, require the use of a nonconventional statistics. We resort to Renyi's approach [19,24–26] as described in Appendix A, and the basic macrovariables in this, say, truncated NCMHT [22,35,37] are

$$h(\mathbf{r},t) = \int d\Gamma\, \hat{h}(\mathbf{r}|\Gamma)\, \bar{P}_\alpha(\Gamma,t) = \int d^3\mathbf{p} \left(\frac{p^2}{2m}\right) f_{1\alpha}(\mathbf{r},\mathbf{p};t), \tag{14}$$

$$n(\mathbf{r},t) = \int d\Gamma\, \hat{n}(\mathbf{r}|\Gamma)\, \bar{P}_\alpha(\Gamma,t) = \int d^3\mathbf{p}\, f_{1\alpha}(\mathbf{r},\mathbf{p};t), \tag{15}$$

$$\mathbf{I}_n(\mathbf{r},t) = \int d\Gamma\, \hat{\mathbf{I}}_n(\mathbf{r}|\Gamma)\, \bar{P}_\alpha(\Gamma,t) = \int d^3\mathbf{p} \left(\frac{\mathbf{p}}{m}\right) f_{1\alpha}(\mathbf{r},\mathbf{p};t), \tag{16}$$

where $f_{1\alpha}$ is the single-particle distribution function

$$f_{1\alpha}(\mathbf{r},\mathbf{p};t) = \int d\Gamma\, \hat{n_1}(\mathbf{r},\mathbf{p}|\Gamma)\, \bar{P}_\alpha(\Gamma|t) \tag{17}$$

and the integration is over phase space.

This nonconventional one-particle Boltzmann-type density distribution function is given in Eq. (A8), and we recall that, according to the theory, it uses the escort probability distribution of order α, i.e., the same as the index of the heterotypical distribution, namely [19,24,35,36],

$$\bar{P}_\alpha(\Gamma|t) = [\bar{\rho}_\alpha(\Gamma|t)]^\alpha \Big/ \int d\Gamma [\bar{\rho}_\alpha(\Gamma|t)]^\alpha, \tag{18}$$

in terms of Renyi's heterotypical distribution of probability $\bar{\rho}_\alpha$, [cf. Eq. (A6)] as described in Appendix A, where the expressions for the basic variables are given [cf. Eqs. (A10), (A15), and (A18)].

The evolution equations for the basic variables in the set (8), derived in the context of a nonlinear kinetic theory

[35,40–42], are

$$\frac{\partial}{\partial t}h(\mathbf{r},t)+\nabla\cdot\mathbf{I}_h(\mathbf{r},t)=J_{h\alpha}(\mathbf{r},t), \tag{19}$$

$$\frac{\partial}{\partial t}n(\mathbf{r},t)+\nabla\cdot\mathbf{I}_n(\mathbf{r},t)=0, \tag{20}$$

$$\frac{\partial}{\partial t}\mathbf{I}_n(\mathbf{r},t)+\nabla\cdot I_n^{[2]}(\mathbf{r},t)=\mathbf{J}_{n\alpha}(\mathbf{r},t)+\mathrm{Im}(\mathbf{r},t), \tag{21}$$

and the nonequilibrium equations of state—which relate the basic variables to the nonequilibrium thermodynamic variables $F_{n\alpha}$, $\vec{F}_{n\alpha}$, and $F_{h\alpha}$—are given in Appendix A. Equation (20) is the conservation equation for the density, and

$$\mathbf{J}_{n\alpha}(\mathbf{r},t)=\int_{-\infty}^{t}dt^{'}e^{\varepsilon(t^{'}-t)}\times\int d\Gamma\{\hat{H}^{'}(\Gamma|t^{'}-t)_0,\{\hat{H}^{'}(\Gamma),\hat{\mathbf{I}}_n(\mathbf{r}|\Gamma)\}\}\bar{P}_\alpha(\Gamma|t) \tag{22}$$

is a collision integral in the Markovian approximation (see Appendix B) accounting for the effect of the collisions generated by $\hat{H}^{'}$, given in the interaction representation, i.e., in $\hat{H}^{'}(t^{'}-t)_0$, where subindex naught indicates the evolution under the dynamics generated by $\hat{H}_0$. The one for the energy in Eq. (19), $J_{h\alpha}$, is identical to the one of Eq. (22) except for the operator density of energy, $\hat{h}$, entering in place of the flux $\hat{\mathbf{I}}_n$. Moreover, $\mathrm{Im}(\mathbf{r},t)$ stands for the force exerted by external sources driving the flow (advection), to be specified in each particular case, and $I_n^{[2]}$ is the second-order flux given by

$$I_n^{[2]}(\mathbf{r},t)=\int d^3p\left[\frac{\mathbf{p}}{m}\frac{\mathbf{p}}{m}\right]\hat{n}_1(\mathbf{r},\mathbf{p}|\Gamma)\bar{P}_\alpha(\Gamma|t)=\int d^3p\left[\frac{\mathbf{p}}{m}\frac{\mathbf{p}}{m}\right]f_{1\alpha}(\mathbf{r},\mathbf{p},t), \tag{23}$$

where $[\mathbf{p}\ \mathbf{p}]$ stands for tensorial product of vectors rendering a rank-2 tensor, which is related to the pressure tensor field [cf. Eq. (28) below]. To solve the system of Eqs. (19) to (21) we need in Eq. (21) to express $I_n^{[2]}$ on the left-hand side in terms of the basic variables [cf. Eq. (28) below].

On the other hand, the collision integral of Eq. (22) consists, in general, of a complicated expression determined by the interactions present in $\hat{H}^{'}$. This is shown in Appendix B [cf. Eq. (B5)], and in what follows we retain the main part of the collision integral [cf. Eq. (B7)], namely

$$\mathbf{J}_{n\alpha}(\mathbf{r},t)\cong-\frac{\mathbf{I}_n(\mathbf{r},t)}{\tau_{I\alpha}}, \tag{24}$$

where $\tau_{I\alpha}$ plays the role of a momentum relaxation time. Differentiating in time Eq. (20), introducing in it Eq. (21), and using it in Eq. (24), we find that

$$\frac{\partial^2}{\partial t^2}n(\mathbf{r},t)=-\nabla\cdot\frac{\partial}{\partial t}\mathbf{I}_n(\mathbf{r},t)=\nabla\cdot\nabla\cdot I_n^{[2]}(\mathbf{r},t)+\nabla\cdot\frac{\mathbf{I}_n(\mathbf{r},t)}{\tau_{I\alpha}}-\nabla\cdot\mathrm{Im}(\mathbf{r},t), \tag{25}$$

which can be rewritten as

$$\tau_{I\alpha}\frac{\partial^2}{\partial t^2}n(\mathbf{r},t)+\frac{\partial}{\partial t}n(\mathbf{r},t)+\nabla\cdot[n(\mathbf{r},t)\mathbf{u}_{\mathrm{ext}}(\mathbf{r},t)]=\tau_{I\alpha}\nabla\cdot\nabla\cdot I_n^{[2]}(\mathbf{r},t), \tag{26}$$

which follows after using Eq. (20), multiplying by $\tau_{I\alpha}$, and introducing the definition

$$\tau_{I\alpha}\nabla\cdot\mathrm{Im}(\mathbf{r},t)\equiv\nabla\cdot[n(\mathbf{r},t)\mathbf{u}_{\mathrm{ext}}(\mathbf{r},t)]\equiv\nabla\cdot\mathbf{I}_{\mathrm{ext}}, \tag{27}$$

in which $\mathbf{u}_{\mathrm{ext}}$ is a quantity with dimension of velocity associated to the external force creating a driven flow, $\mathbf{I}_{\mathrm{ext}}$, in the system (sometimes call solute drag). Next, in order to close Eq. (26) we need to express the second-order flux in terms of the basic variables, n and $\mathbf{I}_n$, which, as described in Appendix A, takes the form [cf. Eq. (A18)]

$$I_n^{[2]}(\mathbf{r},t)=\frac{2}{3m}\zeta_{n\alpha}(\mathbf{r},t)n^{\gamma_\alpha}(\mathbf{r},t)\mathbf{1}^{[2]}+n(\mathbf{r},t)[\mathbf{v}(\mathbf{r},t)\mathbf{v}(\mathbf{r},t)], \tag{28}$$

where it has been used that $\mathbf{I}_n(\mathbf{r},t)=n(\mathbf{r},t)\mathbf{v}(\mathbf{r},t)$, with $\mathbf{v}(\mathbf{r},t)$ being the barycentric velocity field [cf. Eqs. (A15) and (A16)], $\zeta_{n\alpha}$ is given in Eq. (A12), γ_α is the α-dependent power index

$$\gamma_\alpha=\frac{5-3\alpha}{3-\alpha}, \tag{29}$$

$1^{[2]}$ is the unit second-rank tensor, and, according to the results of Appendix A, the possible values of α having physical meaning (i.e., not leading to singularities) belong to the interval

$$0\leqslant\alpha<\tfrac{5}{3}. \tag{30}$$

The appropriate value of α in this interval is to be determined in each case by best fitting of experimental data (for example, see Refs. [5,6,19] and the illustrations in Sec. VII) and according to Eq. (29) it follows that

$$\tfrac{5}{3}\geqslant\gamma_\alpha>0. \tag{31}$$

Substituting Eq. (28) into Eq. (26), we arrive at a nonconventional Maxwell-Cattaneo-like equation for a fluid under flow (advective movement), namely

$$\tau_{I\alpha}\frac{\partial^2}{\partial t^2}n(\mathbf{r},t)+\frac{\partial}{\partial t}n(\mathbf{r},t)-D_{\gamma_\alpha}(\mathbf{r},t)\nabla^2n^{\gamma_\alpha}(\mathbf{r},t)=-\nabla\cdot[n(\mathbf{r},t)\ \mathbf{u}_{\mathrm{ext}}(\mathbf{r},t)]+\tau_{I\alpha}\nabla\cdot\nabla\cdot[n(\mathbf{r},t)[\mathbf{v}(\mathbf{r},t)\ \mathbf{v}(\mathbf{r},t)]]+G_{n\alpha}(\mathbf{r},t), \tag{32}$$

where

$$D_{\gamma_\alpha}(\mathbf{r},t)=\frac{2}{3m}\zeta_{n\alpha}(\mathbf{r},t)\ \tau_{I\alpha}, \tag{33}$$

plays the role of an "anomalous" diffusion coefficient and

$$G_{n\alpha}(\mathbf{r},t)=3m\nabla D_{\gamma_\alpha}(\mathbf{r},t)\cdot\nabla n_{n\alpha}^{\gamma_\alpha}(\mathbf{r},t)+\frac{3m}{2\tau_{I\alpha}}[\nabla^2D_{\gamma_\alpha}(\mathbf{r},t)]n^{\gamma_\alpha}(\mathbf{r},t), \tag{34}$$

a term which is composed of contributions containing the relaxation time $\tau_{I\alpha}$ and the gradient of the coefficient $\zeta_{n\alpha}$, and where we have used that $\mathbf{I}_n(\mathbf{r},t)=n(\mathbf{r},t)\mathbf{v}(\mathbf{r},t)$, [cf. Eq. (A15)].

Taking $\alpha=1$, and then $\gamma_\alpha=1$, Eq. (32) goes over a conventional Maxwell-Cattaneo equation but with sources and for a fluid under flow. The sources, i.e., the right-hand

side term, are composed of the contributions due to the applied external force, the convective pressure (nonlinear in the velocity field), and of the change in space (gradient and Laplacian) of the space- and time-dependent nonconventional diffusion coefficient of Eq. (33). Furthermore, we noted that the kinetic pressure tensor is given by

$$P^{[2]}(\mathbf{r},t) = mI_n^{[2]}(\mathbf{r},t) - mn(\mathbf{r},t)[v(\mathbf{r},t)v(\mathbf{r},t)] = \tfrac{2}{3}u(\mathbf{r},t)\mathbf{1}^{[2]}, \quad (35)$$

as it should, since u is the internal energy density as given by Eq. (A11) in Appendix A. But, because of Eq. (A19) there follows that

$$P^{[2]}(\mathbf{r},t) = \tfrac{2}{3}\,\zeta_{n\alpha}(\mathbf{r},t)n^{\gamma_\alpha}(\mathbf{r},t)\mathbf{1}^{[2]}, \quad (36)$$

with $\zeta_{n\alpha}(\mathbf{r},t)$ given in Eq. (A12), which in the case of $\alpha = 1$ (efficiency and sufficiency satisfied), goes over the standard one of $p = nk_BT$; therefore, Eq. (36) is a nonconventional equation of state for the pressure.

Equation (32) for the density depends on the barycentric velocity, $\mathbf{v}(\mathbf{r},t)$, and then we need to couple it with the equation for the latter, which follows from Eq. (21) once we take into account that $\mathbf{I}_n(\mathbf{r},t) = n(\mathbf{r},t)\mathbf{v}(\mathbf{r},t)$. After some calculations we arrive at an evolution equation for the velocity given by

$$n(\mathbf{r},t)\frac{\partial}{\partial t}\mathbf{v}(\mathbf{r},t) + n(\mathbf{r},t)[\mathbf{v}(\mathbf{r},t)\cdot\nabla]\mathbf{v}(\mathbf{r},t) = -\frac{1}{m}\nabla\cdot P^{[2]}(\mathbf{r},t) - n(\mathbf{r},t)\tau_{I\alpha}^{-1}[\mathbf{v}(\mathbf{r},t) - \mathbf{u}_{\rm ext}(\mathbf{r},t)], \quad (37)$$

with the pressure tensor given in Eqs. (35) and (36).

Returning to Eq. (32), we consider the situation where the motion varies smoothly in time, meaning that the motion is characterized by frequencies such that $\omega\tau_{I\alpha} \ll 1$. Then the first term on the left of Eq. (32) can be neglected and we are left with a "non-Fickian diffusion-advection equation," namely

$$\frac{\partial}{\partial t}n(\mathbf{r},t) - D_{\gamma_\alpha}(\mathbf{r},t)\nabla^2 n^{\gamma_\alpha}(\mathbf{r},t) = -\nabla\cdot[n(\mathbf{r},t)\mathbf{u}_{\rm ext}(\mathbf{r},t)] + \tau_{I\alpha}\nabla\cdot\nabla.[n(\mathbf{r},t)]\,[\mathbf{v}(\mathbf{r},t)\mathbf{v}(\mathbf{r},t)], \quad (38)$$

with D_{γ_α} of Eq. (33), and $G_{n\alpha} = 0$ has been taken, once a weak variation in space of $D_{\gamma_\alpha}(\mathbf{r},t)$ is assumed, and then the terms containing its gradient have been neglected.

We proceed to analyze Eq. (38) and in Sec. VII we present applications to the study of particular systems, including comparison of theory and experiment and where the main points of the theory are further clarified.

III. NON-FICKIAN DIFFUSION

To better visualize the results and characterize the use of the nonconventional approach, we first analyze the simple situation in which no external force is applied, i.e., $u_{\rm ext} = 0$, and then it is assumed that D_{γ_α} is weakly dependent on space and time, that the velocity is small, and the terms containing it in quadratic form can be neglected, all this implying that we can disregard the right-hand side of Eq. (32). Moreover, we consider that the movement occurs in one direction, say x, that is, a long tube where the density is constant in the perpendicular plane as in the case considered in Sec. IV A. (motion in one dimension).

In these conditions, Eq. (32) becomes the nonconventional Maxwell-Cattaneo equation,

$$\tau_{I\alpha}\frac{\partial^2}{\partial t^2}n(x,t) + \frac{\partial}{\partial t}n(x,t) - D_{\gamma_\alpha}\frac{\partial}{\partial x}n^{\gamma_\alpha}(x,t) = 0, \quad (39)$$

and, finally, if the motion is smooth in time, meaning $\omega\tau_{I\alpha} \ll 1$, Eq. (39) becomes approximately the non-Fickian diffusion equation,

$$\frac{\partial}{\partial t}n(x,t) - D_{\gamma_\alpha}\frac{\partial^2}{\partial x^2}n^{\gamma_\alpha}(x,t) = 0, \quad (40)$$

and we recall that $5/3 \geqslant \gamma_\alpha > 0$ [cf. Eq. (31)].

For an initial condition of an impulse type, there follows, after an adaptation of the procedure in Ref. [43], the solution

$$n(x,t) = A_{\gamma_\alpha}^{(\pm)}(t)\left[1 \pm \frac{|\gamma_\alpha - 1|}{3\gamma_\alpha - 1}\frac{x^2}{\sigma_{\gamma_\alpha}^{(\pm)^2}(t)}\right]^{-\frac{1}{1-\gamma_\alpha}}, \quad (41)$$

where the upper plus sign corresponds to the case $\gamma_\alpha < 1$ (then $\alpha > 1$) and the lower minus sign to $\gamma_\alpha > 1$ (then $\alpha < 1$); $\sigma_{\gamma_\alpha}^2(t)$ is the mean-square deviation given by

$$\sigma_{\gamma_\alpha}^{(\pm)^2}(t) = \langle x^2|t\rangle_{\gamma_\alpha}^{(\pm)} = \int dx\; x^2 n(x,t) = \left[a_{\gamma_\alpha}^{(\pm)}\right]^2\frac{|\gamma_\alpha - 1|}{3\gamma_\alpha - 1}t^{2\mu_\alpha}, \quad (42)$$

n_0 is the global density, and

$$a_{\gamma_\alpha}^{(\pm)} = \left[\frac{n_0 L}{I_{\gamma_\alpha}^{(\pm)}}\right]^{-(1-\gamma_\alpha)/(1+\gamma_\alpha)}\left[\frac{|1-\gamma_\alpha|}{2\gamma_\alpha(1+\gamma_\alpha)D_{\gamma_\alpha}}\right]^{1/(1+\gamma_\alpha)}, \quad (43)$$

$$\mu_\alpha = (1+\gamma_\alpha)^{-1} = \frac{1}{4}\left(\frac{3-\alpha}{2-\alpha}\right), \quad (44)$$

$$A_{\gamma_\alpha}^{(\pm)}(t) = \left[\frac{n_0 L}{I_{\gamma_\alpha}^{(\pm)}}\right]\left[\frac{|1-\gamma_\alpha|}{3\gamma_\alpha - 1}\right]^{1/2}\frac{1}{\sigma_{\gamma_\alpha}^{(\pm)}(t)}. \quad (45)$$

Moreover,

$$I_{\gamma_\alpha}^{(+)} = \frac{\Gamma\left(\frac{1}{2}\right)\Gamma\left(\frac{1}{1-\gamma_\alpha} - \frac{1}{2}\right)}{\Gamma\left(\frac{1}{1-\gamma_\alpha}\right)}, \quad (46)$$

for $\gamma_\alpha < 1$, and

$$I_{\gamma_\alpha}^{(-)} = \frac{\Gamma\left(\frac{1}{2}\right)\Gamma\left(\frac{\gamma_\alpha}{\gamma_\alpha - 1}\right)}{\Gamma\left(\frac{\gamma_\alpha}{\gamma_\alpha - 1} + \frac{1}{2}\right)}, \quad (47)$$

for $\gamma_\alpha > 1$.

We note that the integration in space in Eq. (42) has been taken in the interval $0 \leqslant x \leqslant \infty$, whereas the length of the tube is L; therefore, this is a good approximation for time intervals for which the tail of the density is negligible for $x \geqslant L$, typically for $\langle x^2|t\rangle_{\gamma_\alpha}^{(\pm)} \ll L^2$, and then

$$\sigma_{\gamma_\alpha}^{(\pm)2}(t) \sim n_0^{\nu_\alpha}t^{2\mu_\alpha}, \quad (48)$$

where

$$\nu_\alpha = \frac{1-\alpha}{2-\alpha} = 2\,\frac{(\gamma_\alpha - 1)}{(\gamma_\alpha + 1)}. \quad (49)$$

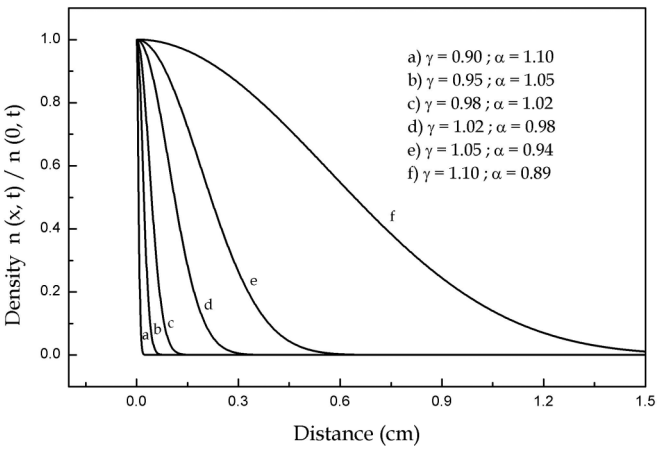

FIG. 1. The concentration profile for $t = 100$ s for several values of exponent γ_α.

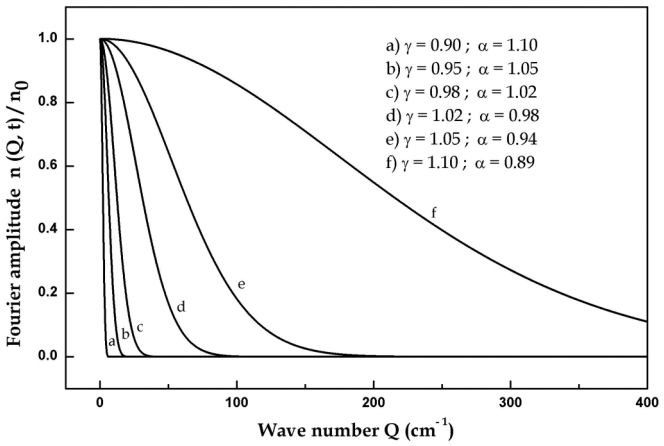

FIG. 2. Fourier amplitude of the concentration profiles of Fig. 1.

Furthermore, considering Eq. (44), we note that, according to the conventional definitions, for $\gamma_\alpha > 1$ it results that $2\mu_\alpha < 1$ and it is said that the motion is subdiffusive, whereas for $\gamma_\alpha < 1$ it follows that $2\mu_\alpha > 1$ and that it is superdiffusive.

In Fig. 1 the profiles of concentration [as given by Eqs. (41) and (42)], for a fixed time $t = 100$ s, and the characteristics of subdiffusion (curves a to c) and superdiffusion (curves d to f) are noted (the normal case, $\alpha = 1$ and $\gamma_\alpha = 1$, is a curve between c and d) are shown. For this illustration we have chosen values of γ_α around 1, i.e., near the strict Fick law, in order to use for D_{γ_α} the unique value of 1.8×10^{-5} cm^2/s, which corresponds to the experimental result described and analyzed in Sec. IV A below. In addition, we used $L = 10$ cm.

The Fourier transform in space of the density of Eq. (41) is

$$n(Q,t) = B_{\gamma_\alpha}^{(+)}\, \tilde{t}^{\,\frac{1}{2(1-\gamma_\alpha)}}\, K_{\frac{1}{2}\frac{(1+\gamma_\alpha)}{(1-\gamma_\alpha)}}\left(\tilde{t}^{\,\frac{1}{1+\gamma_\alpha}}\right), \tag{50}$$

for $\gamma_\alpha < 1$, where $\tilde{t} = \frac{t}{\tau_\gamma}$ with

$$\tau_\gamma^{-1} = \left(a_{\gamma_\alpha}^{(+)}\, Q\right)^{1+\gamma_\alpha}, \tag{51}$$

where $a_{\gamma_\alpha}^{(+)}$ is given in Eq. (43), K_ν is the modified Bessel function of the second kind, and

$$B_{\gamma_\alpha}^{(+)} = \frac{2^{\frac{1}{(\gamma_\alpha-1)}}\, n_0\, L}{\Gamma\left(\frac{1}{2}\right)\Gamma\left(\frac{1}{2}\,\frac{1+\gamma_\alpha}{1-\gamma_\alpha}\right)}. \tag{52}$$

On the other hand,

$$n(Q,t) = B_{\gamma_\alpha}^{(-)}\, \tilde{t}^{\,-\frac{1}{2(\gamma_\alpha-1)}}\, J_{\frac{1}{2}\,\frac{\gamma_\alpha+1}{\gamma_\alpha-1}}\left(\tilde{t}^{\,\frac{1}{1+\gamma_\alpha}}\right), \tag{53}$$

for $\gamma_\alpha > 1$, where J_ν is Bessel function of the first kind and

$$B_{\gamma_\alpha}^{(-)} = 2^{\frac{1}{2}\,\frac{\gamma_\alpha+1}{\gamma_\alpha-1}}\, \Gamma\left(\frac{\gamma_\alpha}{\gamma_\alpha-1}+\frac{1}{2}\right) n_0\, L. \tag{54}$$

Figure 2 shows curves for particular values of γ_α corresponding to Eqs. (50) and (53). We can see that as γ_α becomes smaller than 1 (α larger and larger than 1), the width of the Fourier amplitude continues to increase, as shown in Fig. 3. Moreover, Eqs. (50) and (53) reproduce, to a very good numerical agreement, the results that are alternatively obtained using a Lévy-flight approach, as shown in Sec. VI.

We recall that this is the case of nonconventional diffusion dealt with here using the Renyi approach, which is dependent on the open index α. The standard Fick diffusion equation is a good approximation if the values of Q containing the relevant contributions to $n(\mathbf{Q},t)$ are smaller than a typical cut-off value $Q_{01} \simeq (\bar{v}\tau_1)^{-1}$ where $\bar{v}$ is the root of the mean-square velocity in the movement and τ_1 the momentum relaxation time (Maxwell's characteristic time for the first-order flux). We note that $\bar{v}\tau\, Q$ is the Knudsen number $K_n = \ell/\lambda_n$, where $\ell = \bar{v}\tau_1$ is the mean-free path, and $\lambda_{01} = Q_{01}^{-1}$ is the cut-off wavelength. If such region involves values of Q that are smaller than a cut-off $Q_{12} \simeq (\bar{v}\tau_2)^{-1}$, where now τ_2 is a characteristic time given by $\tau_2^{-1} = \tau_1^{-1} + \theta_2^{-1}$, with θ_2 being Maxwell characteristic time for the second-order flux (the flux related to the pressure tensor), the corresponding hydrothermodynamics leads to an equation of motion of the Maxwell-Cattaneo type, and so on. Therefore, we can define different thermohydrodinamic regimes characterized by a hierarchy of the Knudsen numbers $K_{n_{01}}, K_{n_{12}}$, and so on. This is discussed in Ref. [37].

On the basis of Eq. (42) and, mainly, by inspection of the particular curves considered in Fig. 1, we can see that the nonconventional approach used in the lowest-order

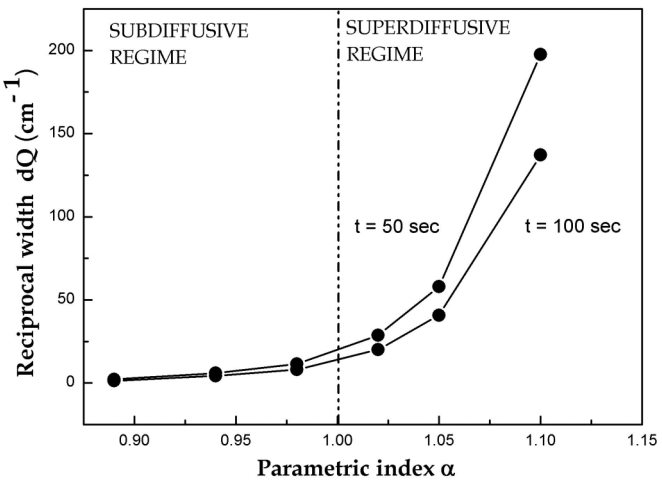

FIG. 3. The width (at height e^{-1} of the maximum amplitude) of the curves of Fig. 2 at $t = 100$ s (lower line) and at $t = 50$ s (upper line) for $Q = 100$ cm^{-1}.

hydrothermodynamics modifies the Gaussian profile resulting from the conventional Fick diffusion equation: For values of α greater than 1 (γ_α smaller than 1), according to Fig. 1 the width of the propagation profile decreases. On the other hand, the width of the propagation profiles continues to increase as index α decreases from the value 1 (γ_α increases from the value 1). In other words, long tails as compared with the one in the normal Fick profile ($\alpha = 1$ and $\gamma_\alpha = 1$) follow for $\gamma_\alpha < 1$ and short tails for $\gamma_\alpha > 1$.

IV. NON-FICKIAN DIFFUSION ADVECTION

Let us consider now the case of non-Fickian diffusion with advection generated by application of an external force, when the movement is governed by Eq. (38), which, after neglecting the term quadratic in the velocities, becomes

$$\frac{\partial}{\partial t} n(\mathbf{r},t) - D_{\gamma_\alpha} \nabla^2 n^{\gamma_\alpha}(\mathbf{r},t) = -\nabla \cdot [n(\mathbf{r},t)\mathbf{u}_{\rm ext}(\mathbf{r},t)]\,. \quad (55)$$

This is a non-Fickian diffusion equation with sources characterized by the term on the right. Such a term has the form of the divergence of a flux, $n(\mathbf{r},t)\ \mathbf{u}_{\rm ext}(\mathbf{r},t)$, imposed on the particles by the external force: The quantity $\mathbf{u}_{\rm ext}(\mathbf{r},t)$, with dimension of velocity, is defined in Eq. (27).

We consider a possible experimental situation in which the movement proceeds in one particular direction, say, along the x axis, and then we have that

$$\frac{\partial}{\partial t} n(x,t) - D_{\gamma_\alpha} \frac{\partial^2}{\partial x^2} n^{\gamma_\alpha}(x,t) + \frac{\partial}{\partial x} [n(x,t) u_{\rm ext}(x,t)] = 0, \quad (56)$$

which can be alternatively written as a continuity-like equation of the form

$$\frac{\partial}{\partial t} n(x,t) + \frac{\partial}{\partial x} I_n^*(x,t) = 0, \quad (57)$$

with

$$I_n^*(x,t) = -D_{\gamma_\alpha} \frac{\partial}{\partial x} n^{\gamma_\alpha}(x,t) + n(x,t) u_{\rm ext}(x,t), \quad (58)$$

composed of the flux associated to the gradient of concentration and the one produced by the external force. Next, we consider two particular cases, labeled A and B.

A. Non-Fickian diffusion under streaming

This case corresponds to take $u_{\rm ext}(x,t) = u_0$, in the x direction. Some instances where this applies are, for example: (1) electrophoresis, the movement in a medium of electrically charged particles under the influence of an electric field, with application in molecular biology (e.g., Ref. [44]); (2) a suspended mixture of one or more types of particles (for example, proteins) in water or other solvent, whereby gravity pulls on each particle with force mg proportional to its mass or a mixture in a centrifuge, where the "centrifugal force" ma_r is also proportional to the particles mass, but the radial acceleration can be much greater than that of gravity [45]; and (3) molecule force experiments *in vitro* which enable the characterization of the mechanical response of biological matter at the nanometer scale [46].

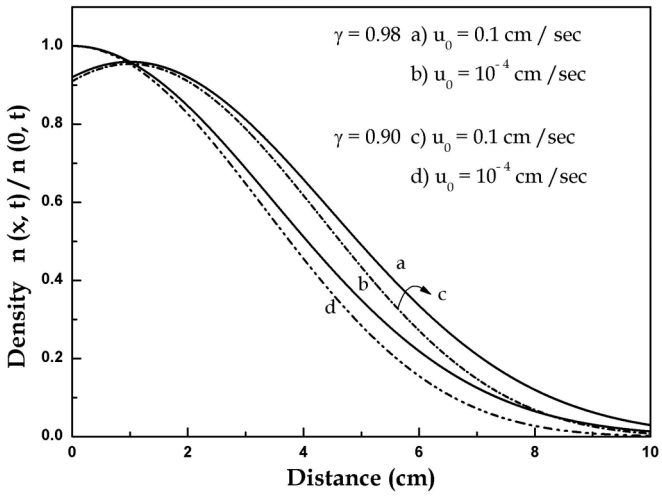

FIG. 4. The concentration profiles for $t = 10$ s for a couple of values of the fractional exponent γ when in conditions of streaming and for a couple of values of quantity u_o, shown in the upper right inset, chosen as indicated in the main text.

In such conditions, the solution of Eq. (56) is

$$n(x,t) = A_{\gamma_\alpha}^{(\pm)}(t) \left[1 \pm \frac{|\gamma_\alpha - 1|}{3\gamma_\alpha - 1} \frac{(x - u_0 t)^2}{\sigma_{\gamma_\alpha}^{(\pm)^2}(t)} \right]^{-\frac{1}{\gamma_\alpha - 1}}, \quad (59)$$

where

$$\sigma_{\gamma_\alpha}^{(\pm)^2}(t) = \langle (x - u_0 t)^2 | t \rangle_{\gamma_\alpha}^{(\pm)} = \frac{|\gamma_\alpha - 1|}{3\gamma_\alpha - 1} \left[a_{\gamma_\alpha}^{(\pm)} \right]^2 t^{2\mu_\alpha} \quad (60)$$

is the mean-square deviation around the peak position $u_o t$, being equal to the one of Eqs. (42). The upper plus and lower minus signs stand as before for the cases $\gamma_\alpha < 1$ and $\gamma_\alpha > 1$, respectively; coefficient $A_{\gamma_\alpha}^{(\pm)}$ is given in Eq. (45) and μ_α in Eq. (44). It can be noted that the flux in Eq. (58) is in this case given by

$$I_n^*(x,t) = n(x,t) u_0 - D_{\gamma_\alpha} \frac{\partial}{\partial x} n^{\gamma_\alpha}(x,t), \quad (61)$$

i.e., the one driven by the external force, with constant velocity u_0, and the diffusive one.

Figure 4 shows the concentration profiles for $t = 10$ s and several values of the exponent γ, using the values of the parameter u_0 indicated in the upper-right inset. We have considered values of γ near 1, and then we have approximated the calculations taking $D_\gamma \simeq D_1 = 1.8 \times 10^{-5}$ cm^2/s (the values considered in Sec. V).

Inspection of Fig. 4 tells us that the movement is the one expected, namely the same profile as in Fig. 1 but with its center of mass displaced by $u_0 t$. Thus, depending on the direction in which the force is applied, there should be, as time elapses, a net tendency to an accumulation of the particles at one of the ends of the container. Moreover, note that the net flow $I_n^*(x,t)$ satisfies an nonconventional Nernst-Planck relation [44]. In fact, in the case where the particles are charged [e.g., biopolymers such as deoxyribonucleic acid and proteins carry ionizable groups, which dissociate on contact with a polar solvent], when placing two parallel plates just outside the solution's container, a distance L apart, with a battery connected to them and maintaining a constant

electrostatic potential difference ΔV, the resulting constant electric field $E_0 = \Delta V/L$ acts on the charges, producing a force qE_0 (q the charge). In this condition we have that $u_0 = \tau_{I_\alpha}(q/m)E_0 = \tau_{I_\alpha}(q\Delta V/mL)$, or $u_0 = qE_0/\zeta_\alpha$, where $\zeta_\alpha^{-1} = \tau_{I_\alpha}/m$ is the so-called viscous friction coefficient, and then Eq. (61) becomes

$$I_n^*(x,t) = n(x,t)\frac{qE_0}{\zeta_\alpha} - D_{\gamma_\alpha}\frac{\partial}{\partial x}n^{\gamma_\alpha}(x,t). \tag{62}$$

In the conventional limit, $\alpha = 1$ and $\gamma = 1$, D_{γ_α} is the conventional diffusion coefficient which is related to the viscous friction coefficient through Einstein relation, and the usual Nernst-Planck formula is recovered,

$$I_n^*(x,t) = D_1\left[\frac{q}{k_BT}E_0 n(x,t) - \frac{\partial}{\partial x}n(x,t)\right], \tag{63}$$

which in the steady-state, taking $I_n^*(ss) = 0$, becomes

$$\frac{d}{dx}ln\ n(x) = \frac{qE_0}{k_BT}. \tag{64}$$

Integrating Eq. (64) along x axis from 0 to L, it follows that

$$ln\frac{n(L)}{n(0)} = \frac{q\Delta V}{k_BT}, \tag{65}$$

which tells us that if we take $q = e$ (the electron charge) and T is the room temperature, say, 300 K, then $e/k_BT \simeq 40\ \mathrm{V}^{-1}$, and for a concentration ratio $\frac{n(L)}{n(0)}$ of the order of 10, it follows that $\Delta V \simeq 60$ mV. Note that many living cells, particularly nerve and muscle cells, maintain a potential across their membranes of a few tens of millivolts. Taking into account that $u_0 = (\tau_{I_\alpha}/m)qE_0$, and using that in the near-normal situation, i.e., γ_α near 1, we can write $D_1 \simeq \tau_I/(m/k_BT)$, considering $D_1 \simeq 2\times 10^5\ \mathrm{cm}^2/\mathrm{s}$ [the case of cetyl-trimethyl-anmmonium bromide (CTAB), discussed in Sec. V A], $q = e$, $T = 300$ K, and then $k_BT/e \simeq (1/40)$ V and $E_0 \simeq 1$ V/cm, there follows the value $u_0 \simeq 8\times 10^{-6}$ cm/s. Thus, the values used in Fig. 4 correspond to values of E_0 (in the above conditions) of, roughly, 1 and 15 V, respectively. It can be noted that in the case of streaming flow there is no modification of the profile of the density in motion in the sense that the time dependence of the mean-square deviation around the peak position remains unaltered [cf. Eqs. (42) and (60)].

B. Non-Fickian diffusion under harmonic force

This case corresponds to taking $u_{\mathrm{ext}}(x) = -x/\tau_0$, where τ_0 is a constant with the dimension of time, leading to Ornstein-Uhlenbeck dynamics [47]. Available experimental situations can be, for example, charged particles in an electric field increasing linearly along direction x. Another possibility consists in using laser tweezers to produce an optical trap. An optical trap is formed when micron-sized transparent particles whose index of refraction is greater than that of the surrounding medium is located within a focused laser beam. The refracted rays differ in intensity over the volume of the sphere and exert a pico-Newton-scale force on the particle, drawing it towards the region of the highest light intensity. The optical trap is harmonic near the focal point and the trapping constant, τ_0^{-1} above, can be tuned by adjusting the laser power [48]. This has been used for studying ribonucleic acid (RNA) folding [49] and in the study of adhesion of biological cells it is used molecule force spectroscopy where it is created a "springlike" (harmonic) potential [50].

In this case we have that

$$I_n^*(x,t) = -n(x,t)\frac{x}{\tau_0} - D_{\gamma_\alpha}\frac{\partial}{\partial x}n^{\gamma_\alpha}(x,t), \tag{66}$$

and the solution of Eq. (57) for an initial Gaussian-like perturbation at $x = 0$ and with mean-square displacement σ_0^2 is, for $\gamma_\alpha < 1$, given by

$$n(x,t) = n(0,t)\left[1 + \frac{1-\gamma_\alpha}{3\gamma_\alpha - 1}\frac{x^2}{\left[\sigma_{\gamma_\alpha}^{(+)}\right]^2}\right]^{-\frac{1}{1-\gamma_\alpha}}, \tag{67}$$

where

$$n(0,t) = \frac{n_o L}{I_{\gamma_\alpha}^{(+)}\sigma_{\gamma_\alpha}^{(+)}(t)}\left(\frac{1-\gamma_\alpha}{3\gamma_\alpha - 1}\right)^{1/2}, \tag{68}$$

$$\left[\sigma_{\gamma_\alpha}^{(+)}(t)\right]^2 = \sigma_0^2\left[\left(1-\Delta_{\gamma_\alpha}\right)\exp(-(1-\gamma_\alpha)(t/\tau_0)) + \Delta_{\gamma_\alpha}\right]^{\frac{2}{1+\gamma_\alpha}}, \tag{69}$$

$$\Delta_{\gamma_\alpha} = 2\gamma_\alpha\tau_0 D_{\gamma_\alpha}\frac{z_{0\gamma_\alpha}^{1-\gamma_\alpha}}{(3\gamma_\alpha - 1)\sigma_0^2}, \tag{70}$$

$$\frac{1}{z_{0\gamma_\alpha}} = \frac{2n_0 L}{I_{\gamma_\alpha}^{(+)}}\frac{(1-\gamma_\alpha)^{1/2}}{(3\gamma_\alpha - 1)^{1/2}}\frac{1}{\sigma_0}, \tag{71}$$

and the integral $I_{\gamma_\alpha}^{(+)}$ is given in Eq. (46).

In Fig. 5 we consider the cases of $\tau_0 = 0.01$ s and 1.0 s, $\gamma_\alpha = 0.98$, which is near the normal condition when $\gamma_\alpha = 1$, and we have approximated D_{γ_α} by $D_1 \simeq 1.8\times 10^{-5}\ \mathrm{cm}^2/\mathrm{s}$ as in Sec. IV A, and this value was also used for $\gamma_\alpha = 0.9$. Moreover, we have taken $\sigma_0^2 = 0.1\ \mathrm{cm}^2$ and $L = 10$ cm. Since $u_{\mathrm{ext}} < 0$, the imposed flux opposes the diffusion of the particles, as expected once the first contribution on the right is negative and the second positive, being, respectively, the flux generated by the action of the external force and the one generated by the thermodynamic force.

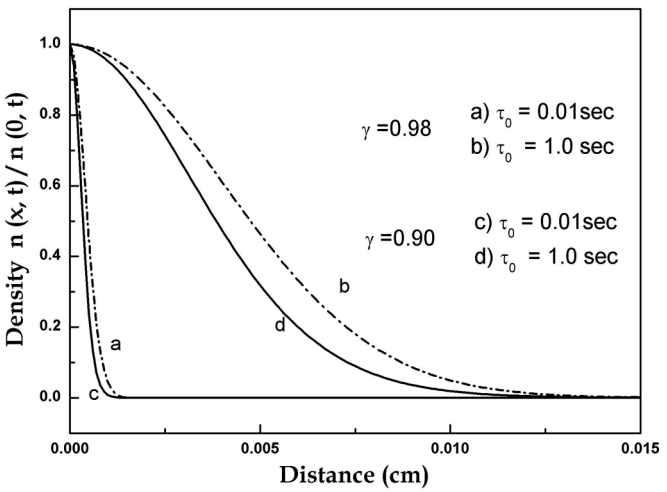

FIG. 5. Profiles of the concentration (at time $t = 10$ s under the influence of two values of the flux imposed by the external harmonic force).

The values for τ_0 we have used were chosen on the basis that, in modulus, the force $(m/\tau_I)(x/\tau_0)$, when we consider values of γ near 1, can be rewritten as $(1/\beta D\tau_0)x$. Taking the end point $x = L$ and using $T_0 = 300$ K and $D \simeq 2 \times 10^{-5}$ cm^2/s (the case of CTAB; see the previous section and Sec. IV A), when $\beta D \simeq 5 \times 10^9$ s/gr, if we impose that the force has the value of 1 pN, a typical value using optical traps [48], it follows that $\tau_0 \simeq 0.2$ s. Hence, the values used in Fig. 5 correspond to, roughly, having fixed end forces of 20 and 0.2 pN.

According to Fig. 5 the root of the mean-square deviation, $\langle x^2\rangle^{1/2}$ at $t = 1$ s, is ∼16 cm for the case $\tau_0 = 1.0$ s and ∼0.06 cm for $\tau_0 = 0.01$ s.

The mean-square deviation is given in Eq. (69) and it can be noted that for large t, i.e., $t \gg \tau_0$, the mean-square deviation is practically a constant and the motion is between super- and subdiffusion. We can see that differently to the case of streaming flow, the time dependence of the mean-square deviation is greatly influenced by the flow driven by a harmonic force [cf. Eqs. (42) and (69)].

V. THE STEADY STATE

Since the external force, represented by $u_{\rm ext}(x)$, is time independent, after a transient has elapsed, a steady state sets in, $\partial I_n^*/\partial t = 0$, and, consequently, I_n^* is a constant which is taken as zero [45]. Hence, from Eq. (58) it follows that

$$D_{\gamma_\alpha}\frac{\partial}{\partial x}n^{\gamma_\alpha}(x) - u_{\rm ext}(x)n(x) = 0, \tag{72}$$

whose solution for $\gamma_\alpha < 1$ is

$$n(x) = A_\alpha\left[1 - (1-\gamma_\alpha)\,v(x)\right]^{-\frac{1}{1-\gamma_\alpha}}, \tag{73}$$

where

$$v(x) = \left(\gamma_\alpha A_\alpha^{\gamma_\alpha - 1}D_{\gamma_\alpha}\right)^{-1}\int_o^x dx' u_{\rm ext}(x'), \tag{74}$$

and A_α is determined by the conditions that the integration in space of $n(x)$ is the given whole concentration n_0.

Let us consider the case

$$u_{\rm ext}(x) = u_0 - \frac{x}{\tau_0}, \tag{75}$$

that is, a combination of motion under streaming discussed in Sec. IV A and under the harmonic force discussed in Sec. IV B.

Introducing Eq. (75) into Eq. (74) we have that

$$v(x) = \left(\gamma_\alpha A_\alpha^{\gamma_\alpha - 1}D_{\gamma_\alpha}\right)^{-1}\left(u_0 x - \tfrac{1}{2}\tau_0^{-1}x^2\right) \tag{76}$$

and then

$$n(x) = A_\alpha\Big[1 - (1-\gamma_\alpha)\left(\gamma_\alpha A_\alpha^{\gamma_\alpha-1}D_{\gamma_\alpha}\right)^{-1} \times \left(u_0 x - \tfrac{1}{2}\tau_0^{-1}x^2\right)\Big]^{-\frac{1}{1-\gamma_\alpha}}. \tag{77}$$

We analyze this profile for the two cases we have considered, items *A* and *B* in Sec. IV.

A. Constant force: Streaming flow

In the case of streaming flow, when $u_{\rm ext}(x) = u_0$, of Sec. IV A, the steady-state concentration is given by

$$n(x) = n(0)\left[1 - (1-\gamma_\alpha)\kappa_{\gamma_\alpha}x\right]^{-\frac{1}{1-\gamma_\alpha}}, \tag{78}$$

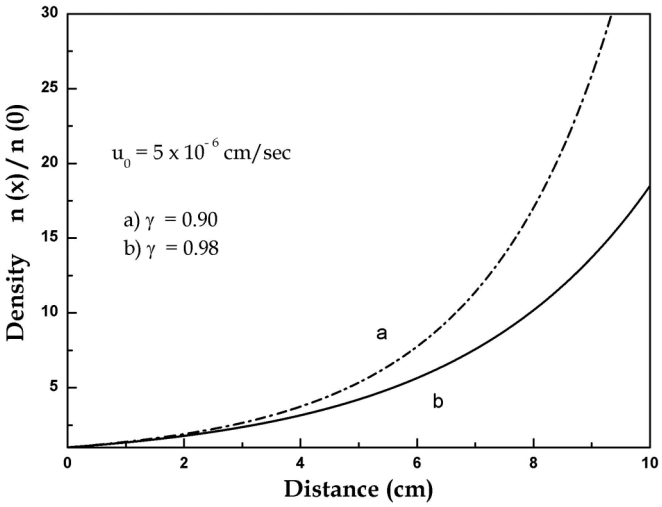

FIG. 6. Profiles of the steady-state density as given by Eq. (78).

for $\gamma_\alpha < 1$ (then $\alpha > 1$), where

$$n_0 = n(0)\;{}_2F_1\left(\frac{1}{1-\gamma_\alpha}; 1, 2, \kappa_{\gamma_\alpha}L\right), \tag{79}$$

with ${}_2F_1$ being the Gauss hypergeometric function, and

$$\kappa_{\gamma_\alpha} = \left[\frac{n^{1-\gamma_\alpha}(0)}{\gamma_\alpha D_{\gamma_\alpha}}\right]u_0, \tag{80}$$

which has the dimension of the reciprocal of distance. It can be noted that in the normal case, i.e., $\gamma_\alpha = 1$, $\kappa_1 = u_0/D_1$ and

$$n(0) = n_0\frac{u_0 L}{D_1}[\exp(u_0 L/D_1) - 1]^{-1}. \tag{81}$$

Inspection of Eq. (78) tells us that in the steady state the particles are redistributed in such a way that there is an accumulation at the boundary in $x = L$. This is a result of the balance that sets in over time between the flux due to the diffusive effects and the flux (stream) forced by the external force.

This is illustrated in Fig. 6, where we have used values of γ near 1, so, as before, we can introduce the approximation $D_\gamma \simeq D_1 = 1.8 \times 10^{-5}$ cm^2/s and $\kappa_{\gamma_\alpha} \simeq u_0/\gamma_\alpha D_1$.

B. Harmonic force: Ornstein-Uhlenbeck dynamics

In the case of motion under a harmonic force, $u_{\rm ext} = -x/\tau_0$, discussed in Sec. IV B, the steady state shows the concentration profile

$$n(x) = n(0)\left[1 + (1-\gamma_\alpha)\left(\frac{x}{\Lambda_{\gamma_\alpha}}\right)^2\right]^{-\frac{1}{1-\gamma_\alpha}} \tag{82}$$

for $\gamma_\alpha < 1$ (then $\alpha > 1$), where

$$\Lambda_{\gamma_\alpha}^2 = \gamma_\alpha n^{(\gamma_\alpha - 1)}(0)D_{\gamma_\alpha}\tau_0, \tag{83}$$

and $n(0)$ follows from the condition whereby the total number of particles is given, i.e.,

$$n_0 L = n(0)\int_0^L dx\left[1 + (1-\gamma_\alpha)\left(\frac{x}{\Lambda_{\gamma_\alpha}}\right)^2\right]^{-\frac{1}{1-\gamma_\alpha}}. \tag{84}$$

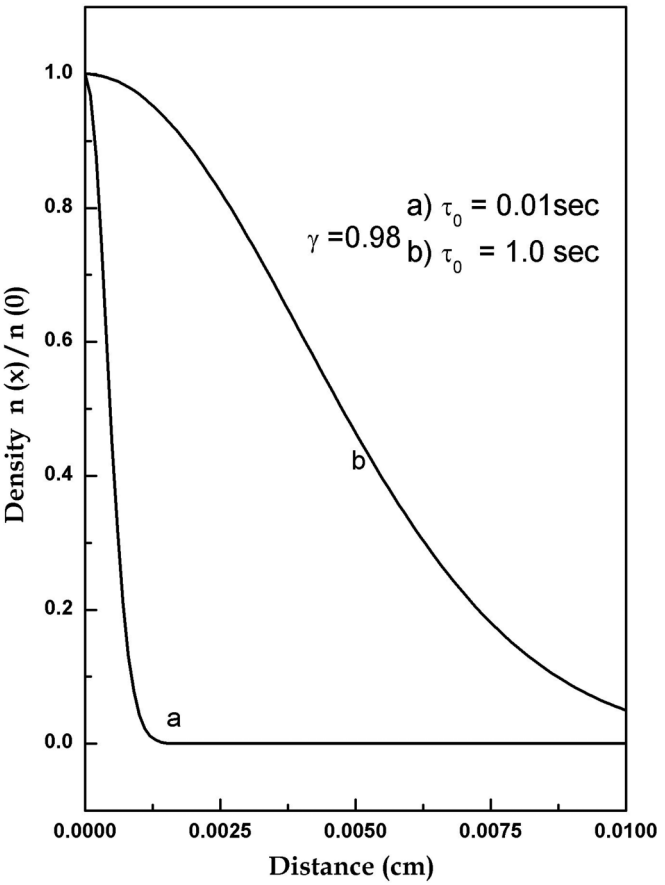

FIG. 7. Profiles of the steady-state density as given by Eq. (82).

This is illustrated in Fig. 7, where, as before, we have taken values of γ near 1, so the approximation $D_\gamma \simeq D_1 = 1.8 \times 10^{-5}$ cm^2/s can be used and $\Lambda_{\gamma_\alpha} \simeq \gamma_\alpha D_1 \tau_0$.

VI. NON-FICKIAN DIFFUSION AS A LÉVY PROCESS

At this point it is worth noting that, in 1937, the *Lévy distribution* and *Lévy processes* were introduced (see, for example, Ref. [51]). They have had a strong impact on different areas of scientific analysis, including physics, economics, econometrics, dynamical systems, and chaotic dynamics. In the kind of dynamical systems we are considering here, it has been noticed [52] that some problems of hydrodynamic motion in solutions of polymers, micelles, and others—some considered in the next section—can be related to Lévy processes. In the case of non-Fickian diffusion, which we have described above, it can be proved that, in fact, the result we have obtained for the Fourier amplitudes of the density, i.e., $n(Q,t)$, shown in Fig. 2 and given in Eqs. (50) and (53), practically coincides with the characteristic function of the Lévy process, namely

$$f_\eta(\mathbf{Q},t) = \exp\{-C_\eta(t)|\mathbf{Q}|^\eta\}, \tag{85}$$

with C_η being a constant and η a fractional power. This is illustrated in Fig. 8 for three particular cases.

Moreover, it has been shown [53] that a Maxwell-Cattaneo equation is the continuum limit of a persistent random walker. The spectrum of such an equation reproduces almost exactly,

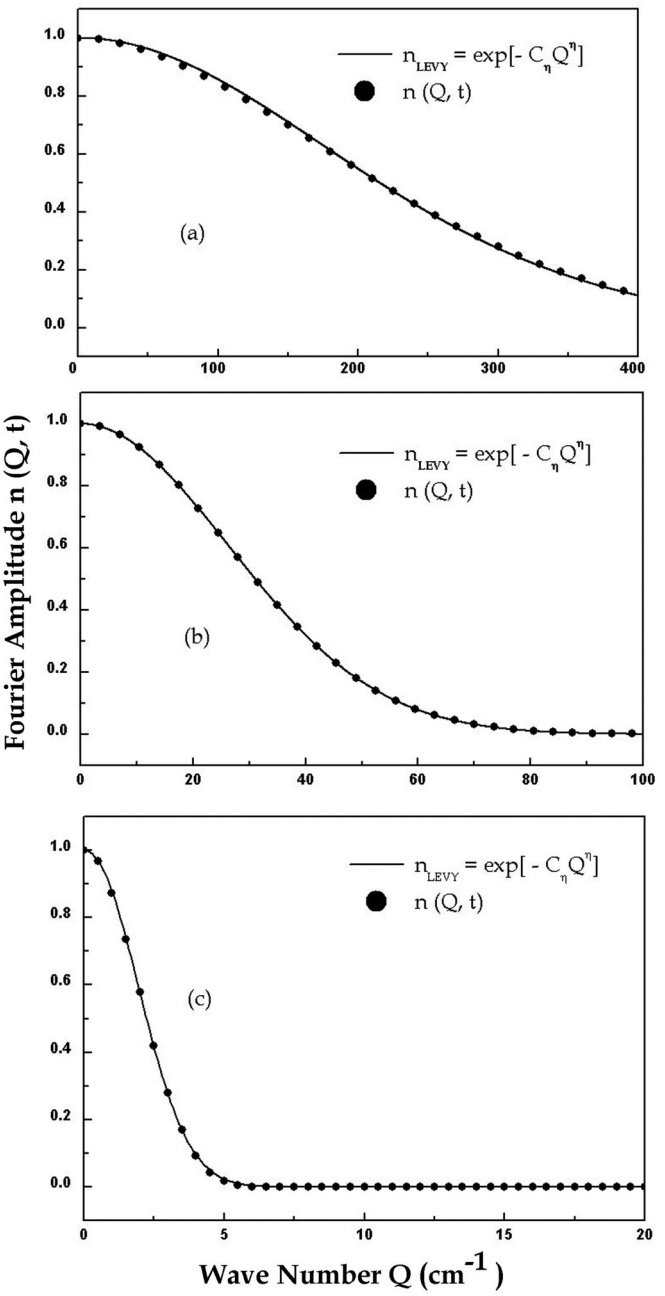

FIG. 8. (a) Dependence of Fourier amplitude vs wave number for $\gamma_\alpha = 1.10$ and $\alpha = 0.89$ where the full line is Lévy distribution and circles correspond to $n(\mathbf{Q},t)$ of Eq. (53). In this case, $C_\eta = 7.7 \times 10^{-4} \pm 2.96 \times 10^{-7}$ and $\eta = 1.98 \pm 1.1 \times 10^{-4}$. (b) Dependence of Fourier amplitude vs wave number for $\gamma_\alpha = 0.98$ and $\alpha = 1.02$ where the full line is Lévy distribution and the circles correspond to $n(\mathbf{Q},t)$ of Eq. (50). In this case, $C_\eta = 4 \times 10^{-5} \pm 2 \times 10^{-7}$ and $\eta = 1.831 \pm 9.7 \times 10^{-4}$. (c) Dependence of Fourier amplitude vs wave number for $\gamma_\alpha = 0.90$ and $\alpha = 1.10$ where the full line is Lévy distribution and circles correspond to $n(\mathbf{Q},t)$ of Eq. (50). In this case, $C_\eta = 1.285 \times 10^{-1} \pm 8 \times 10^{-5}$ and $\eta = 2.09 \pm 5.8 \times 10^{-4}$.

for all wavelengths, the spectrum of the original, discrete process.

Besides the Gaussian profile in the normal diffusion process, a great number of phenomena follow a Gaussian distribution. However, it has been noticed that there are cases

where, instead of Gaussian tails, there are so-called inverse-power-law tails (e.g., the case of nonconventional diffusion of Sec. III, with an application to solutions of micelles presented in next section). Paul Lévy developed formal statistical models that yielded such tails [54].

Lévy considered distributions of sums of independent random variables (see, for example, Refs. [51,54,55]) and posed the following question: What is the most general form of probabilities $P_j(X;t)$ of the random variable X with the property that, if $P_1(X;t)$ and $P_2(X;t)$ have the same form of the characteristic function, the one for the compound probability will also have that form? Lévy found the general form for the characteristic function to be essentially the one of Eq. (85).

The distribution of Eq. (85) can be derived in the framework of the maximum entropy formalism (MaxEnt) [56] from the maximization of its Shannon informational entropy,

$$S_S(t) = -\int d^3Q f_\eta(\mathbf{Q};t) ln f_\eta(\mathbf{Q};t), \tag{86}$$

subjected to the constraint of normalization,

$$\int d^3Q f_\eta(\mathbf{Q};t) = 1, \tag{87}$$

and the *nonconventional constraint of a fractional moment*, namely

$$M_\eta(t) = \int d^3Q |\mathbf{Q}|^\eta f_\eta(\mathbf{Q};t). \tag{88}$$

As shown in Fig. 7, the non-Gaussian tails in the nonconventional diffusion process can be equivalently described by (1) a Renyi statistical approach in which the distribution follows by applying MAXENT to Renyi informational entropy or (2) a standard statistical approach in which the distribution follows by applying MAXENT to Shannon informational entropy but introducing nonconventional constraints (Lévy's fractional moment).

It can also be noted [54] that long tails may imply self-similar scaling and that a Lévy flight is a random walk in the continuum, with jumps governed by a Lévy's distribution of jumps lengths, and Rosenau [53] showed that the continuum limit of a persisting random walker is a Maxwell-Cattaneo-like equation. Moroever, Jespersen *et al*., considering Lévy flight subjected to an external force field, in what they call an anomalous transport process, using a Langevin equation with Lévy noise, derived an "anomalous" diffusion equation similar to the NCMHT presented here [57].

VII. AN ILLUSTRATIVE EXAMPLE

We stress that in so-called soft-matter [2], polymers and surfactants in solutions, the transport of particles is strongly influenced by the variety of aggregation of macromolecules with a distribution of configurations and masses involving dangling ends, bottlenecks, and backbends present in the disordered structure (forming a fractal lattice) and where also breakup and recombination of such aggregates occur. Therefore, one cannot expect movement that can be accounted for by Fickian diffusion. As noted, a way to deal with such situations may be the one previously described as nonconventional hydrothermodynamics, a tentative solution to circumvent the difficulty of not having access to the whole of the relevant information that the problem at hand requires. Moreover, we are not facing a nonconventional behavior shown by a few "strange" fluids but rather a typical situation for fluids containing an arrangement of molecules exhibiting fractal-like structures [4]). We consider, as an illustration of application of the theory, the case of micelles, namely aggregates of amphiphilic molecules in water with, eventually, added salts. They may be present in multiple shapes: spheres, rods, disks, and wormlike micelles sometimes called "living polymers" [57–59]. In the case of the latter, the so-called nonconventional diffusion was interpreted in terms of a Lévy flight theory [52] (cf. previous section).

We analyze here self-diffusion measurements of elongated micelles in a semidilute regime [59], resorting to the Renyi-approach-based hydrothermodynamic theory so far presented. The experimental procedure, with a description of the experimental setup, is given in that reference. The micelles are CTAB ($C_{16}H_{33}NCH_3Br$ with $m \simeq 5 \times 10^{-25}$ Kg), with the concentration of C in an aqueous solution with added KBr. In the experiment a diffusion movement along, say, the x direction is expected. The experimental method allows us to measure the mean-square x component of displacement as a function of time $\langle x^2|t\rangle$. In the case of Fickian diffusion, $\langle x^2|t\rangle = Dt$, where D is the diffusion coefficient, and in the experiment $\ell^2/\tau_r = \tau_r^{-1}[\langle x^2|t+\tau_r\rangle - \langle x^2|t\rangle] = D$ is measured, where ℓ^2 is the square of the fringe where it is observed the change in the luminescent spectrum coming from the micelles labeled with fluorescent probes, and τ_r is the recovery time of the signal. The value of D is obtained, which is independent of the concentration of the solute. The study is usually restricted to a thin two-dimensional sheet within the bulk flowing system, but tentative solutions to follow the motion throughout the whole fluid volume are underway (streams traced by speckle) [60].

On other hand, for complex structured systems displaying non-Fickian diffusion, as is the case in the experiment of Ref. [58], the mean-square deviation given in Eq. (42) shows a dependence on the concentration of the solute. In such case, a nonconventional diffusion coefficient can be defined—the quantity that is measured in the experiment—and is given by $\tilde{D}_{\gamma_\alpha} = \tau_r^{-1}[\langle x^2|t+\tau_r\rangle_{\gamma_\alpha} - \langle x^2|t\rangle_{\gamma_\alpha}]$, which is solute-concentration dependent, that is, $\tilde{D}_{\gamma_\alpha} \sim C^{\nu_\alpha}$, with ν_α of the Eq. (48).

Differing from the conventional case, we can see that this pseudodiffusion coefficient depends on a fractional power of the concentration and that in the limit of α going to 1 we recover the standard result of kinetic theory for a Fickian diffusion. It has been noted [61] that we have to keep in mind that *fractional power-law behaviors may be purely apparent or simply transient or spurious*. Moreover [62], the situation becomes even worse when going to real-life phenomena (differing from idealized fractal systems). It seems that many of the observed scaling laws are just artifacts or transients. In the case where spurious scaling in models can be simulated with very high precision, it should be noted that not every power law supposedly seen in nature is a real power law. The log-normal distribution used in biology shows an apparent power-law behavior, and the same applies to its

use in finance [61], and others arise in different areas, e.g., the dependence of mobility on concentration in the case of nonlinear transport in semiconductors [63].

Evidently, in a log-log presentation of $\tilde{D}_\alpha$ vs C, as is reported in Fig. 2 of Ref. [58], ν_α is given by the tangent to the curve at each point, i.e.,

$$\nu_\alpha = \frac{d\,[\log\,\tilde{D}_\alpha]}{d\,[\log\,C]}, \tag{89}$$

and then it is dependent on the value of the concentration of C, as will be shown below. The measurements were performed by changing the salinity (concentration of KBr) and varying the concentration of the CTAB. It can be noted that only at very dilute concentrations C of CTAB is a constant diffusion coefficient in accord with a Fickian diffusion observed. But as the concentration increases, for each salinity level the value of the pseudodiffusion coefficient decreases, with a tendency of $\log\,\tilde{D}$ versus $\log\,C$, with $\nu_\alpha < 0$ and depending on the concentration of the salt, to display itself in a straight line. This fractional power law, giving a rapid decrease in $\tilde{D}$, is observed when the concentration is increased above a limiting value of C^*, which may be indicating a particular increase in the complex behavior of the system of micelles when the effects in the aggregation of the macromolecules become strong, as noted at the beginning of this section. Therefore, once $\nu_\alpha < 0$, according to the experimental results, it then follows that $\alpha > 1$ (but $<5/3$), $\gamma_\alpha < 1$, and $\xi_\alpha > 1$, where $\xi_\alpha = 2\mu_\alpha$ of Eq. (37), implying the so-called subdiffusion; these indexes are given in Eqs. (49), (29), and (44), i.e., respectively,

$$\nu_\alpha = \frac{1-\alpha}{2-\alpha}; \quad \gamma_\alpha = \frac{5-3\alpha}{3-\alpha}; \quad \xi_\alpha = 2\mu_\alpha = \frac{1}{2}\frac{(3-\alpha)}{(2-\alpha)}. \tag{90}$$

In the case of the experimental results of Ref. [58], we consider those of the pseudo-diffusion coefficient $\tilde{D}$ versus the molar concentration C of CTAB for the case of a salinity (concentration of KBr) of 0.25 M, and $T_0 = 300$ K, and where C^* (concentration at the region where the degree of complexity seems to have a steep change) is $\sim$0.02 M. The value of ν_α is derived [cf. Eq. (89)] from the slope in the figure displaying the experimental data (Fig. 2 in Ref. [58]), and using the relations in Eq. (90); the resulting values of α, γ_α, and ξ_α are shown in Table I.

We recall that in the experiment the mean-square deviation in the time-interval τ_r (the recovery time of the luminescent signal) is determined. Concerning the value of α, we stress that it depends on the system's dynamics, size and geometry, boundary conditions, structure, the macroscopic-thermodynamic state of the system, and the experimental protocol [19]. Moreover, on the basis of the results in the works of Refs. [5,6], it is expected that α approximately depends on the molar concentration C as

$$\alpha(C) \simeq \frac{C^{-1} + C_1^{-1}}{C^{-1} + C_2^{-1}}, \tag{91}$$

where $C_1^{-1} \simeq 125\,\mathrm{M}^{-1}$ and $C_2^{-1} \simeq 75\,\mathrm{M}^{-1}$, which follows from best fitting of the values of Table I to the expression of this Eq. (91), graphically described in Fig. 9. We can see that as C decreases, going over the situation of a very dilute solution, index α tends to 1, as expected, once we would have a fluid with small (or none) aggregates of macromolecules, while for increasing C index α increases, implying an ever increasing complexity in the micelles structure, going over its limiting value of 5/3, as it should.

Some authors [58] report that using de Gennes reptation model there follows the value $\nu_r = -1.75$, when we would have $\gamma \simeq 0.1$ and $\alpha \simeq 1.6$ (approaching the limit $5/3 = 1.66$), indicating a relatively high level of complexity. Moreover, the connection of d_f, the average fractal dimension, and α is empirically determined in the experiments involving nonconventional diffusion in the study of fractal-structured electrodes in microbatteries [6]. Here we do not have an access to that information, but on the basis of the analysis done in

TABLE I. The values of ν_α from the experimental data; from these follow the values of the others according to Eq. (90).

C (M)	ν_α	α	γ_α	ξ_α
0.001	−0.15	1.13	0.86	1.07
0.0025	−0.16	1.14	0.85	1.08
0.005	−0.33	1.25	0.71	1.16
0.02	−1.29	1.56	0.22	1.63
$\geqslant$0.03	−1.4	1.58	0.18	1.69

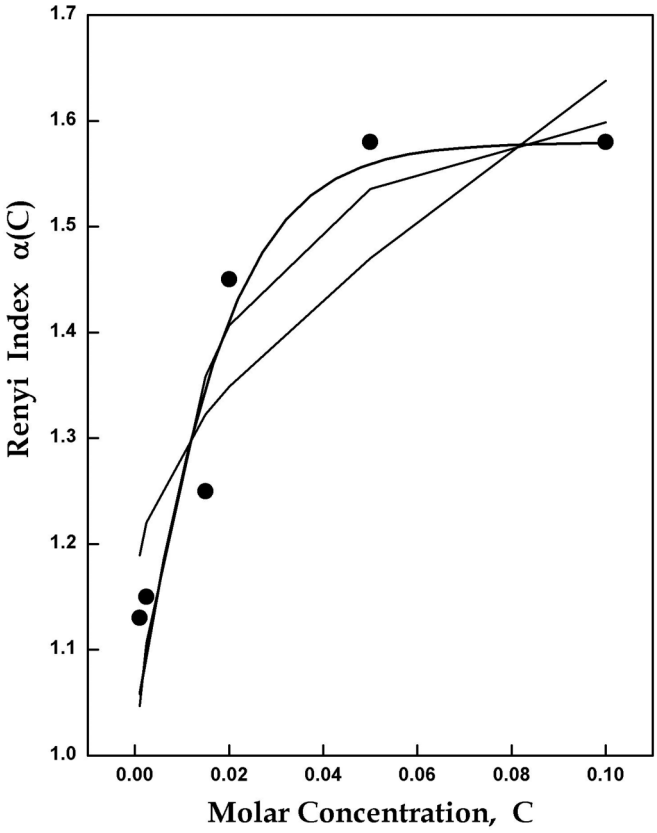

FIG. 9. Dependence of index α on the molar concentration of the micelles. Dots are the values of α given in Table I derived from the experimental data and the full curve drawn using Eq. (91).

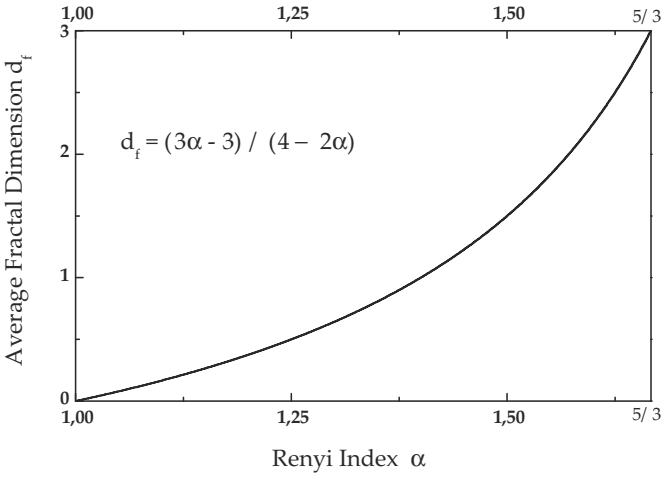

FIG. 10. The conjectured average fractal dimension vs the index α [the dependence of the latter on the molar concentration of the micelles is given in Fig. (1) and adjusted by Eq. (92)]. Note that d_f changes from 0 to 3 as α varies in the permitted interval $1 \leqslant \alpha < 5/3$ and then $1 \geqslant \gamma_\alpha > 0$ and $\xi_\alpha > 1$ corresponding to a superdiffusive regime.

Ref. [6] we conjecture the possible relation

$$d_f(\alpha) = \frac{3}{2}\frac{\alpha - 1}{2 - \alpha} \tag{92}$$

or

$$\alpha = \frac{4d_f + 3}{2d_f + 3}. \tag{93}$$

According to Eq. (92) and using Table I, we can see that in the limit of very dilute solutions ($C \to 0$ and $\alpha \to 1$ it follows that $d_f \to 0$ (presence of a very few amphiphilic molecules) and for very large concentration [$C \gg C_1$ and C_2 in Eq. (91) and $\alpha \to 5/3$], we find that $d_f \to 3$, the three-dimensional space occupied by a continuous uniform mass of molecules. We recall that this is not a geometrical (or pure) fractal dimension but a kind of measure of the degree of the structural complexity of the micelles characteristics and distribution in the solution. Figure 10 shows the change of that average fractal dimension with the power index α of Table I.

The theory applies well to the cases, as those considered here, where the saline concentration is larger than 0.1 M. For lower values it cannot account for concentrations $C > C^*$, the point at which there is a kind of change of regime with a somewhat sharp decrease in $\tilde{D}$ with increasing concentration. It is worth noting that they correspond to values of ν_α beyond the one in de Gennes reptation theory. In the former conditions a high salinity may indicate more frequent collisions than in the latter situation, a more efficient breaking of the micelles, leading to simpler aggregates and then to a less complex general structure, which allows the theory to provide satisfactory results. In the conditions of low salinity and values of C larger than C^*, there appears to be present a high level of complexity in the overall structure. This indicates the necessity of an extension of the hydrothermodynamic theory, namely to further incorporate the second-order flux, which implies adding the pressure-tensor field to the basic variables, which, for example, may show relevant effects in the case of fluids under high levels of flow [30,31]. In that way shear stress is introduced, which can make the movement more complex.

VIII. DISCUSSION AND CONCLUDING REMARKS

As noted, when dealing with fluids showing a fractal-like structure, we face difficulties in describing their hydrodynamic behavior because the complex structure strongly affects the motion. Once we do not have accessible information to properly include in the *hidden constraints* related to the characteristics of this internal structure the theoretical treatment, it is worth exploring the use of nonconventional statistical mechanical methods, particularly introducing a nonconventional nonequilibrium statistical ensemble formalism. NCNESEF is used to derive a nonconventional kinetic equation (or nonconventional generalized Boltzmann equation) from which are derived the nonconventional hydrodynamic equations of nonconventional mesoscopic hydrothermodynamics (i.e., those for the densities of particles and of energy and their fluxes of all orders), which we described in Sec. II. The standard MHT of any order, as noted, is described in Ref. [21] at the classical level and (in the physics of semiconductors) in Refs. [38,39] at the quantum level. They follow on the application of the generalized Boltzmann kinetic equation (classical [22] or Peierls-Boltzmann-like equation in the quantum (phonons) case [38,39]). To obtain the nonconventional one, we need to introduce, for example, the Renyi distribution (see Appendix A).

For illustration we have applied it, using the Renyi approach, for the study of the hydrodynamic motion of fractal-like-structured fluids starting at a low-order description, namely the one in terms of a first-order mesoscopic hydrothermodynamics. We arrived at a nonconventional Maxwell-Cattaneo-like hydrothermodynamic equation involving a fractional power law, characterized by an exponent related to the index α of Renyi nonconventional statistics. This index is to be determined by best fitting with the experimental data [5,6,19]. As already noted, it is, in principle, influenced by the system's dynamics, geometry and size, boundary conditions, structure, thermodynamic state, and even by the experimental protocol. In that sense it consists not of a fully closed theory, but of a particularly sophisticated and useful method for a study of systems in the presence of hidden constraints.

However, even though we do not have in that way a complete physical picture of the problem at hand the sophistication of the formalism allows us to obtain some insight into the physical aspects of the situation. On the one hand, the use of the escort probability takes care of introducing correlations (fluctuations and higher-order variances), and, on the other hand, the nonconventional probability distribution (the Renyi one here) modifies the weight of the Fourier amplitudes $n(\mathbf{Q})$ of the density in relation to their conventional values (cf. Fig. 2). As already noted, classical hydrothermodynamics together with Fick's diffusion equation is a satisfactory approach while $n(\mathbf{Q})$ has leading contributions for small Q; otherwise we need to introduce higher-order NCMHT [22,35,37].

A particular limit of a nonconventional Maxwell-Cattaneo equation [cf. Eq. (32)] provides a nonconventional Fickian

diffusion-advection equation (movement under driven flow), cf. Eq. (38), both coupled to the evolution equation for the first flux [or barycentric velocity, cf. Eq. (37)], which has been dealt with in detail in Sec. III.

Other approaches specifically dealing with non-Fickian diffusion have been addressed by several authors. Some are based on Hvadra-Charvat [64] nonconventional statistics (which is shown to be equivalent to the Renyi one [23,26]), e.g., Refs. [65,66]; Solokov *et al*. resort to fractional kinetics [67]; Zumofen uses a so-called probabilistic continuous-time random-walk approach [68]; and Bologna *et al*. claim an exact analytical treatment in a density approach to ballistic anomalous diffusion [69].

Concerning the work on non-Fickian diffusion based on Hvrada-Charvat nonconventional statistics, sometimes referred to as Tsallis statistics, in Refs. [65,66], we stress—and the same applies to Renyi statistics and many others [23]—that the "entropies" on which they are based are not physical entropies (and are not "observable entropies") but just auxiliary generating functions in theoretical statistics to provide nonconventional statistics when, in conjunction with the use of escort probabilities, applying them to problems that present "hidden constraints." On this it is worth mentioning the words of Edwin Thompson Jaynes [70], "there exists a persistent failure to distinguish between the informational entropy, which is a property of any probability distribution, and the experimental entropy of thermodynamics which is instead a property of a thermodynamic state: Many research papers are flawed fatally by the authors' failure to distinguish between these entirly different things." We call attention to the fact that the illustration we presented here (non-Fickian diffusion and diffusion-advection) is an application of a nonconventional approach to mesoscopic hydrothermodynamics of only order 1.

In Sec. IV we considered two examples, namely motion under streaming, as in the case of electrophoretic methods (Sec. IV A), and motion under the influence of a harmonic force, as in the case of the use of optical traps (Sec. IV B). The influence of the flow on the non-Fickian diffusion has been evidenced, and the mutual coupling of flow and kinetic effects exerting a restructuring influence has been discussed.

Moreover, for further illustration of the matter we have considered and analyzed, within the framework of the theory, experiments on diffusion of micelles in solution. Diffusion of micelles (Sec. VII) displays non-Fickian features evidenced by the "anomalous" behavior of the mean-square displacement. The experimental results were fitted, allowing us to determine the degree of complexity in the system, which, as expected, increases with the concentration. The reptation model of de Gennes and the Lévy flight approach are encompassed in this theory.

We may also mention another interesting case, this one in biophysics, namely "anomalous" diffusion of single molecules in living cells [71]. We disagree with the authors [70] on their statement that the observations pose fundamental questions for statistical mechanics and reshapes the views on cell biology. It seems to be another example of the difficulties introduced by the presence of "hidden constraints," that is, hydrodynamic motion of, in this case, the single molecules in a complex medium, probably of fractal on average structure [4–6,19]. Thus, of course, normal Brownian motion cannot be expected, the experiments showing a mean-square deviation with a power law with an exponent [our ν_α of Eq. (90)] smaller than 1 and, hence, that messenger RNA diffusion *in vivo* has a weaker time dependence than the standard Brownian diffusion.

ACKNOWLEDGMENTS

The authors acknowledge the financial support received from the São Paulo State Research Foundation, FAPESP (A.R.V., J.G.R., and R.L.). D.J. and J.C.V. acknowledge the financial support from the Dirección General de Investigación of the Spanish Ministry of Economy and Competitiveness under Grant FIS2012-32099 and of the Direcció General de Recerca of the Generalitat of Catalonia under Grant No. 2009-SGR-00164.

APPENDIX A: THE SINGLE-PARTICLE DISTRIBUTION IN RENYI STATISTICS

Let us take the one-particle dynamical operator $\hat{n}_1$ of Eq. (13) as a basic variable, and then the corresponding Renyi statistical operator is [19]

$$\bar{\rho}_\alpha(\Gamma|t) = \frac{1}{Z_\alpha(t)}\Big[1-(1-\alpha)\int d^3r\, d^3p\, \varphi_{1\alpha}(\mathbf{r},\mathbf{p};t) \times (\hat{n}_1(\mathbf{r},\mathbf{p}|\Gamma) - f_{1\alpha}(\mathbf{r},\mathbf{p};t))\Big]^{\frac{1}{1-\alpha}}, \tag{A1}$$

where φ_1 is the Lagrange multiplier (nonequilibrium thermodynamic variable) associated to $\hat{n}_1$, and

$$f_{1\alpha}(\mathbf{r},\mathbf{p};t) = \int d\Gamma \hat{n}_1(\mathbf{r},\mathbf{p}|\Gamma)\bar{P}_\alpha(\Gamma|t), \tag{A2}$$

with $\bar{P}_\alpha$ being the escort probability given in Eq. (11). Moreover, $Z_\alpha(t)$ ensures the normalization that is

$$Z_\alpha(t) = \int d\Gamma\Big[1-(1-\alpha)\int d^3r\, d^3p\, \varphi_{1\alpha} \times (\mathbf{r},\mathbf{p};t)\hat{n}_1(\mathbf{r},\mathbf{p}|\Gamma)\Big]^{\frac{\alpha}{1-\alpha}}. \tag{A3}$$

Introducing the modified Lagrange multiplier

$$\tilde{\varphi}_{1\alpha}(\mathbf{r},\mathbf{p};t) = \frac{\varphi_{1\alpha}(\mathbf{r},\mathbf{p};t)}{\lambda_{1\alpha}(\mathbf{r},\mathbf{p};t)}, \tag{A4}$$

where

$$\lambda_{1\alpha}(\mathbf{r},\mathbf{p};t) = 1+(1-\alpha)\int d^3r\, d^3p\, \varphi_{1\alpha}(\mathbf{r},\mathbf{p};t) f_{1\alpha}(\mathbf{r},\mathbf{p};t), \tag{A5}$$

the statistical operator of Eq. (A1) takes the form

$$\bar{\rho}_\alpha(\Gamma|t) = \frac{1}{\tilde{Z}_\alpha(t)}\Big[1-(1-\alpha)\int d^3r\, d^3p\, \tilde{\varphi}_{1\alpha} \times (\mathbf{r},\mathbf{p};t)\, \hat{n}_1(\mathbf{r},\mathbf{p}|\Gamma)\Big]^{1/(1-\alpha)}. \quad \text{(A6)}$$

where $\tilde{Z}_\alpha(t)$ provides the normalization of $\bar{\rho}_\alpha$.

As shown elsewhere [35,72], one can rewrite this statistical operator in the form of a generalized grand-canonical one, when the basic variables are independent combinations of $\hat{n}_1$ consisting of the densities of energy and of particles and their fluxes of all order. As stated in Sec. II, we are resorting to a truncated version consisting of keeping only the variables $\hat{h}$, $\hat{n}$, and $\hat{\mathbf{I}}_n$ of Eqs. (10) to (12), which is accomplished by approximating $\tilde{\varphi}_1$ in the form

$$\tilde{\varphi}_{1\alpha}(\mathbf{r},\mathbf{p};t) = F_{n\alpha}(\mathbf{r},t) + \mathbf{F}_{n\alpha}(\mathbf{r},t)\cdot\frac{\mathbf{p}}{m} + F_{h\alpha}(\mathbf{r},t)\frac{p^2}{2m}. \quad \text{(A7)}$$

Introducing this expression in the statistical operator of Eq. (A6), and the resulting one in the escort probability $\bar{P}_\alpha$ in Eq. (A2), and performing the calculations, it follows that

$$f_{1\alpha}(\mathbf{r},\mathbf{p};t) = A_\alpha(t)\Big\{1-(1-\alpha)\Big[F_{n\alpha}(\mathbf{r},t) + \mathbf{F}_{n\alpha}(\mathbf{r},t).\frac{\mathbf{p}}{m} + F_{h\alpha}(\mathbf{r},t)\frac{p^2}{2m}\Big]\Big\}^{\alpha/(1-\alpha)}, \quad \text{(A8)}$$

where

$$A_\alpha(t) = \frac{N}{\int d^3r\, d^3p\, [1-(1-\alpha)\,\tilde{\varphi}_1(r,p,t)]^{\frac{\alpha}{1-\alpha}}}, \quad \text{(A9)}$$

where N is the number of particles and $\tilde{\varphi}_1$ is the one of Eq. (A7).

This $f_{1\alpha}$ is a single-particle distribution function (for $\alpha = 1$ becomes the usual Boltzmann one) which, we stress, is the one associated with the use of the truncated description in terms of the variables h, n, and $\mathbf{I}_n$. Introducing this distribution function in Eq. (14) to (16) and performing the calculation, we obtain that

$$h(\mathbf{r},t) = u(\mathbf{r},t) + n(\mathbf{r},t)\tfrac{1}{2}mv^2(\mathbf{r},t). \quad \text{(A10)}$$

In Eq. (A10)

$$u(\mathbf{r},t) = \zeta_{n\alpha}(\mathbf{r},t)n^{\gamma_\alpha}(\mathbf{r},t) \quad \text{(A11)}$$

is the internal energy, where

$$\zeta_{n\alpha}(\mathbf{r},t) = \left(\frac{3}{5-3\alpha}\right)\left[\frac{F_{h\alpha}^{3/2}(\mathbf{r},t)}{2\pi\; I_{1/2}(\alpha)(2m)^{3/2}A_\alpha(t)}\right]^{\gamma_\alpha-1} \times \frac{1}{F_{h\alpha}(\mathbf{r},t)}, \quad \text{(A12)}$$

with $\gamma_\alpha - 1 = 2(1-\alpha)/(3-\alpha)$.

$$I_{\frac{1}{2}}(\alpha) = (1-\alpha)^{-\frac{3}{2}}\frac{\Gamma\left(\frac{3}{2}\right)\Gamma\left(\frac{1}{\alpha-1}\right)}{\Gamma\left(\frac{3}{2}+\frac{1}{1-\alpha}\right)} \quad \text{(A13)}$$

for $1 \leqslant \alpha < 5/3$, and

$$I_{\frac{1}{2}}(\alpha) = (1-\alpha)^{-\frac{3}{2}}\frac{\Gamma\left(\frac{3}{2}\right)\Gamma\left(\frac{\alpha}{\alpha-1}\right)-\frac{3}{2}}{\Gamma\left(\frac{\alpha}{\alpha}-1\right)} \quad \text{(A14)}$$

for $0 < \alpha \leqslant 1$, and Γ is the Gamma function. Moreover,

$$\mathbf{I}(\mathbf{r},t) = n(\mathbf{r},t)\mathbf{v}(\mathbf{r},t), \quad \text{(A15)}$$

after introducing the definition

$$\mathbf{F}_{n\alpha}(\mathbf{r},t) = F_{h\alpha}(\mathbf{r},t)\mathbf{v}(\mathbf{r},t), \quad \text{(A16)}$$

with $\mathbf{v}(\mathbf{r},t)$ playing the role of the barycentric velocity field, and, for the second-order flux of Eq. (24), it follows that

$$I_n^{[2]}(\mathbf{r},t) = \int d^3p\left[\frac{\mathbf{p}}{m}\frac{\mathbf{p}}{m}\right] f_{1\alpha}(\mathbf{r},\mathbf{p};t) = \frac{2}{3m}u(\mathbf{r},t)1^{[2]} + n(\mathbf{r},t)\,[\mathbf{v}(\mathbf{r},t)\mathbf{v}(\mathbf{r},t)], \quad \text{(A17)}$$

and, using Eq. (A11), we have that

$$I_n^{[2]}(\mathbf{r},t) = \frac{2}{3m}\,\zeta(\mathbf{r},t)\,n^{\gamma_\alpha}(\mathbf{r},t)1^{[2]} + n(\mathbf{r},t)\,[\mathbf{v}(\mathbf{r},t)\mathbf{v}(\mathbf{r},t)]. \quad \text{(A18)}$$

We recall that the pressure tensor field is related to the second flux by [cf. Eq. (35)]

$$P^{[2]}(\mathbf{r},t) = mI_n^{[2]}(\mathbf{r},t) - mn(\mathbf{r},t)[\mathbf{v}(\mathbf{r},t)\mathbf{v}(\mathbf{r},t)] = \tfrac{2}{3}\,u(\mathbf{r},t)1^{[2]} = \tfrac{2}{3}\,\zeta_{n\alpha}(\mathbf{r},t)\,n^{\gamma_\alpha}(\mathbf{r},t)1^{[2]}, \quad \text{(A19)}$$

which is an "anomalous" equation of state, going, for $\alpha = 1$, over the "normal" one, $p = nk_BT$.

APPENDIX B: COLLISION INTEGRAL

The collision integral of Eq. (22) is calculated for the case of the fluid of N particles of mass m embedded in the second fluid of N_R particles of mass M acting as a thermal bath at fixed temperature T_R, with both systems interacting through a central force potential. The Hamiltonian is

$$\hat{H} = \hat{H}_S + \hat{H}_B + \hat{H}', \quad \text{(B1)}$$

where $\hat{H}'$ is the interacting energy

$$\hat{H}' = \sum_{j,\mu}\upsilon(|\mathbf{r}_j - \mathbf{R}_\mu|). \quad \text{(B2)}$$

($\mathbf{r}_j$ and $\mathbf{R}_\mu$ refer to the coordinates of particles in the system and in the bath, respectively). Moreover, $\hat{H}_S$ and $\hat{H}_B$ are the Hamiltonians of the system and of the thermal bath, that is, the kinetic energies plus the internal potential interactions. We consider a dilute solution, large average separation between the particles, thus allowing us to neglect the interaction between them and then in Eq. (B1) we have

$$\hat{H}_S + \hat{H}_B = \sum_{j=1}^{N}\frac{p_j^2}{2m} + \sum_{\mu=1}^{N_R}\frac{P_\mu^2}{2M} + \frac{1}{2}\sum_{\mu\neq\nu}w(\mathbf{R}_\mu - \mathbf{R}_\nu), \quad \text{(B3)}$$

that is, the kinetic energy of the particles in the solute and the kinetic energy of the particles of the solvent plus their pair interaction. We resort to the Markovian approximation [35,40] and then we have that

$$\mathbf{J}_n(\mathbf{r},t) \simeq \int_{-\infty}^{t} dt'\, e^{\varepsilon(t'-t)}\int d\Gamma\{\hat{H}'(\Gamma|t'-t)_0, \{\hat{H}'(\Gamma),\hat{\mathbf{I}}_n(\Gamma|\mathbf{r},t)\}\}\bar{P}_\alpha(t,0)\rho_R, \quad \text{(B4)}$$

where subindex zero in $\hat{H}'(t'-t)_0$ indicates evolution in the interaction representation, and we use for the statistical distribution of the thermal bath, ρ_R, a canonical one with temperature T_R. Note that the approximate (Markovian) scattering integral of Eq. (B4) is quadratic in the interaction strength and corresponds to the classical limit of the golden rule of mechanics, and we recall that $\{\ldots,\ldots\}$ stands for the Poisson bracket.

The lengthy but straightforward calculation of Eq. (B4) provides several contributions to this scattering integral: one involving the gradient of concentration (leading to a modification of the diffusion coefficient due to the collisions) and the other involving the gradient of the quasitemperature (implying in a cross-effect between thermal and material motion). Another one is related to correlation effects in space of the collisional processes (i.e., nonlocal effects), which has the very peculiar characteristic that results in an interaction between pairs of particles mediated by the interaction of these particles with those of the bath [22] (this has been shown to occur between two Brownian particles embedded in a thermal bath [73]; another typical example is the one in type I superconductivity, with the electron-phonon interaction leading to the formation of Cooper pairs). These two contributions are neglected; when considering a dilute solution, the most relevant one that can be interpreted as a Maxwell-relaxation effect [21] is given by

$$\mathbf{J}_{n\alpha}(\mathbf{r},t) \simeq -\frac{n_R n}{m m_r}\sqrt{\frac{\pi}{2}}(M\beta_R)^{\frac{3}{2}}\sum_{\mathbf{q}}|\upsilon(\mathbf{q})|^2\frac{[\mathbf{qq}]}{q}\,\mathbf{A}_\alpha(\mathbf{r},\mathbf{q};t), \tag{B5}$$

where $\upsilon(\mathbf{q})$ is the Fourier transform of the interaction potential of Eq. (B2) between the two types of particles; $[\ldots]$ stands for tensorial product of vectors; m_r is the reduced mass, $m_r^{-1} = m^{-1} + M^{-1}$; $\beta_R = 1/k_B T_R$ is the reciprocal of the temperature of the thermal bath; and n and n_R are the global densities of particles in the system and in the thermal bath, respectively. Moreover,

$$\mathbf{A}_\alpha(\mathbf{r},\mathbf{q},t) = \int d^3p\,\frac{\mathbf{p}}{m}\exp\left\{-\beta_R\frac{M}{2m^2q^2}(\mathbf{q}\cdot\mathbf{p})^2\right\} f_{1\alpha}(\mathbf{r},\mathbf{p};t), \tag{B6}$$

where $f_{1\alpha}(\mathbf{r},\mathbf{p},t)$—the single-particle distribution function in the Renyi approach—is given in Eq. (A8).

As shown elsewhere [22], expanding the exponential present in Eq. (B6), we obtain an expression of the form

$$\mathbf{A}_\alpha(\mathbf{r},\mathbf{q};t) = -\frac{1}{\tau_{I_\alpha}}\mathbf{I}_n(\mathbf{r},t) + \mathbf{R}(\mathbf{r};t), \tag{B7}$$

where $\mathbf{R}$ is a series of terms involving the odd-rank fluxes, i.e., $I^{[3]}$, $I^{[5]}$, etc., and τ_{I_α} is the relaxation time of the flux (and of the linear momentum density of the particles) given by

$$\tau_{I_\alpha}^{-1} = \frac{n_R}{mM}\sqrt{\frac{\pi}{2}}(M\beta_R)^{3/2}\int dq\; q^3|\upsilon(\mathbf{q})|^2. \tag{B8}$$

Since we are working in a truncated description that neglects the influence of the fluxes that are higher than the first one, $\mathbf{R}$ is discarded and then Eq. (24) follows. Note that in the given conditions it is possible to approximate the collision integral associated to the interaction between the particles in the solute in a relaxation time approximation. The τ_{I_α} in Eq. (24) then is to be interpreted as given by the Matthiessen rule introducing a new $\tau_{I_\alpha}^*$ such that $(\tau_{I_\alpha}^*)^{-1} = \tau_{I_\alpha}^{-1} + \tau_{p_\alpha}^{-1}$, with τ_{p_α} being the relaxation time for particle-particle collisions.

[1] S. Hawling and D. Ben Avraham, Adv. Phys. **36**, 695 (1987).

[2] T. A. Witten, Rev. Mod. Phys. (Supplement Centenary APS) **71**, S367 (1999); T. A. Witten and P. A. Pincus, *Structured Fluids: Polymers, Colloids, Surfactants* (Oxford University Press, Oxford, UK, 2004); J. R. Dutcher and A. G. Marangoni, *Soft Materials* (Marcel Dekker, New York, 2005).

[3] J. Crank, *The Mathematics of Diffusion* (Oxford University Press, Oxford, UK, 1975).

[4] F. Family and T. Vicsek, *Dynamics of Fractal Surfaces* (World Scientific, Singapore, 1991).

[5] A. R. Vasconcellos, E. Laureto, E. A. Meneses, and R. Luzzi, J. Mod. Phys. B **18**, 1743 (2004); Chaos Solitons Fractals **28**, 8 (2006).

[6] J. G. Ramos, A. Gorenstein, M. U. Kleinke, T. G. Souza Cruz, and R. Luzzi, J. Mod. Phys. B **20**, 4121 (2006).

[7] P. N. Prasad, J. E. Mark, and T. J. Fai (eds.), *Polymers and Other Advanced Materials: Emerging Technologies and Bussiness Oportunities* (Plenum, New York, 1996).

[8] W. R. Salaneck, K. Seki, A. Kahn, and J. J. Pireaux (eds.), *Conjugated Polymers and Molecular Interfaces: Science and Technology for Photonic and Optoelectronic Applications* (Marcel Dekker, New York, 2001).

[9] M. J. Bowden and S. R. Turner, Editors, *Polymers for High Technology: Electronics and Photonics* (American Chemical Society, Washington, DC, 1987).

[10] C. P. Wong, *Polymers for Electronics and Photonic Applications* (Academic Press, San Diego, 1993).

[11] E. Reichmanis and J. H. O'Donnell (eds.), *The Effects of Radiation on High-Technology Polymers* (American Chemical Society, Washington, DC, 1989).

[12] Y. Lu, *Solitons and Polarons in Conducting Polymers* (World Scientific, Singapore, 1988).

[13] A. J. Heeger, S. Kivelson, J. R. Schrieffer, and W. P. Su, Rev. Mod. Phys. **60**, 781 (1988).

[14] T. Anderson and S. Roth, Braz. J. Phys. **24**, 746 (1994).

[15] D. de Kee and K. F. Wissbrum, Physics Today **51**, 24 (1998).

[16] J. P. Bouchaud and A. Georges, Phys. Rep. **195**, 127 (1990).

[17] S. L. Keller, P. Boltenhagen, D. J. Pine, and J. A. Zasadzinski, Phys. Rev. Lett. **80**, 2725 (1998).

[18] S. P. Sullivan, A. J. Sederman, M. L. Johns, and L. F. Gladden, J. Non-Newtonian Fluid Mech. **143**, 59 (2007); S. P. Sullivan *et al.*, Science **316**, 955 (2007).

[19] R. Luzzi, A. R. Vasconcellos, and J. G. Ramos, Rivista Nuovo Cimento **30**, 95 (2007).

[20] T. Dedeurwaerdere, J. Casas-Vazquez, D. Jou, and G. Lebon, Phys. Rev. E **53**, 498 (1996).

[21] R. Luzzi, A. R. Vasconcellos, and J. G. Ramos, *Informational Statistical Thermodynamics* (Teubner-Bertelsmann Springer, Stuttgart, 2000); D. Jou, J. Casas-Vázquez, and G. Lebon, *Extended Irreversible Thermodynamics*, 4th ed. (Springer, Berlin, 2010); G. Lebon, D. Jou, and J. Casas-Vázquez, *Understanding Non-equilibrium Thermodynamics* (Springer, Berlin, 2008).

[22] C. A. Bomfim, J. G. Ramos, A. R. Vasconcellos, and R. Luzzi, J. Stat. Phys. **143**, 1020 (2011).

[23] J. N. Kapur and H. K. Kesavan, *Entropy Optimization Principles with Applications* (Academic Press, San Diego, 1992).

[24] A. Renyi, Proc. 4th Berkeley Symp. Math. Stat. Problems **1**, 547 (1961).

[25] A. Renyi, *Probability Theory* (North-Holland, Amsterdam, The Netherlands, 1970), Chap. IX, p. 540 et seq.

[26] P. Jizba and T. Arimitsu, Ann. Phys. **312**, 17 (2004).

[27] A. E. English, T. Tanaka, and E. R. Edelman, J. Chem. Phys. **107**, 1645 (1997).

[28] R. Smith, J. Fluid Mech. **105**, 469 (1981); **175**, 201 (1987); **182**, 447 (1987).

[29] M. F. Schlesinger, G. M. Zavslasky, and J. Klafter, Nature **363**, 31 (1993).

[30] D. Jou, J. Casas-Vázquez, and M. Criado-Sancho, *Thermodynamics of Fluids Under Flow* (Springer, Berlin, 2001).

[31] V. Garzó and A. Santos, *Kinetic Theory of Gases in Shear Flow* (Kluwer Academic, Dordrecht, The Netherlands, 2003).

[32] Y. Han *et al*., Science **314**, 626 (2006).

[33] R. P. Taylor, Sci. Am. **287**, 116 (2002).

[34] J. Eggers, in *A Perspective Look at Nonlinear Media*, edited by J. Parisi *et al*. (Springer, Berlin, 1998), p. 305; S. Hess, in *ibid*., p. 75.

[35] R. Luzzi, A. R. Vasconcellos, and J. G. Ramos, *Predictive Statistical Mechanics: A Nonequilibrium Ensemble Formalism* (Kluwer Academic, Dordrecht, The Netherlands, 2002); R. Luzzi, A. R. Vasconcellos, and J. G. Ramos, Rivista Nuovo Cimento **30**, 95 (2007).

[36] C. Beck and F. Schlögel, *Thermodynamics of Chaotic Systems* (Cambridge University Press, Cambridge, UK, 1993).

[37] A. R. Vasconcellos, A. R. B. Castro, A. C. B. Silva, R. Luzzi, AIP Advances **3**, 072106 (2013).

[38] C. G. Rodrigues, A. R. Vasconcellos, and R. Luzzi, Eur. J. Phys. B **86**, 200 (2013).

[39] J. G. Ramos, A. R. Vasconcellos, and R. Luzzi, J. Chem. Phys. **112**, 2692 (2000).

[40] L. Lauck, A. R. Vasconcellos, and R. Luzzi, Physica A **168**, 789 (1990).

[41] A. I. Akhiezer and S. V. Peletminski, *Methods of Statistical Physics* (Pergamon, Oxford, UK, 1981).

[42] A. L. Kuzemsky, Int. J. Mod. Phys. B **21**, 2821 (2007).

[43] J. P. Pascal and H. Pascal, Physica A **208**, 351 (1994); J. Stephenson, *ibid*. **222**, 234 (1995).

[44] P. Nelson, *Biological Physics: Energy, Information, Life* (Freeman, New York, 2004); L. A. Lewis, in *Medical Physics, Vol. III*, edited by O. Glasser (Year Book Publishers, Chicago, 1960); J.-L. Viovy, Rev. Mod. Phys. **72**, 813 (2000).

[45] R. K. Hobbie, *Intermediate Physics for Medicine and Biology* (Springer, New York, 1997).

[46] M. Sotomayor and K. Schulten, Science **316**, 1144 (2007).

[47] G. E. Uhlenbeck and L. S. Ornstein, Phys. Rev. **36**, 823 (1930).

[48] A. Askin, Proc. Natl. Acad. Sci. USA **94**, 4853 (1997).

[49] J. Liphardt, B. Onoa, S. B. Tinoco, and C. Bustamante, Science **292**, 733 (2001).

[50] E. A. Evans and D. A. Calderwood, Science **316**, 1148 (2007).

[51] G. M. Zavslasky, Phys. Rep. **371**, 461 (2002).

[52] A. Ott, J. P. Bouchaud, D. Langevin, and W. Urbach, Phys. Rev. Lett. **65**, 2201 (1990); J. P. Bouchaud, A. Ott, D. Langevin, and W. Urbach, J. Phys. II France **1**, 1465 (1991).

[53] P. Kolodner, Phys. Rev. E **48**, R665 (1993).

[54] E. W. Montroll and M. F. Shlesinger, J. Stat. Phys. **32**, 209 (1983)

[55] M. F. Schlesinger, G. M. Zavslaski, and U. Frush (eds.), *Lèvy Flights and Related Topics in Physics* (Springer, Berlin, 1985).

[56] P. T. Landsberg, in *Problems in Thermodynamics and Statistical Physics*, edited by P. T. Landsberg (Pion, London, 1971).

[57] S. Jespersen, R. Metzler, and H. C. Fogedby, Phys. Rev. E **59**, 2736 (1999).

[58] D. Brockmann, L. Hufnagel, and T. Geisel, Nature **439**, 462 (2006).

[59] R. Messager, A. Ott, D. Chatenay, W. Urbach, and D. Langevin, Phys. Rev. Lett. **60**, 1410 (1988).

[60] L. Lèger, H. Hernet, and F. Rondelez, Macromolecules **14**, 1732 (1981).

[61] N. Boccara, *Modeling Complex Systems* (Springer, New York, 2004).

[62] P. Grassberger, New J. Phys. **4**, 17 (2002).

[63] C. G. Rodrigues, A. R. Vasconcellos, and R. Luzzi, Phys. Status Solidi B **246**, 417 (2009).

[64] J. Hvrada and F. Charvat, Kybernetica **3**, 30 (1967); see also Ref. [23].

[65] C. Tsallis, Braz. J. Phys. **29**, 1 (1999).

[66] A. R. Plastino and A. Plastino, Phys. Lett. A **222**, 347 (1995).

[67] I. M. Sokolov *et al*., Phys. Today **55**, 48 (2002).

[68] G. Zumofen and J. Klafter, Phys. Rev. E **47**, 851 (1993).

[69] M. Bologna *et al*., J. Math. Phys. **51**, 043303 (2010).

[70] E. T. Jaynes, *Probability Theory: The Logic of Science* (Cambridge, University Press, Cambridge, UK, 2002).

[71] E. Barkai, Y. Garini, and R. Meltzler, Phys. Today **65**, 29 (2012).

[72] D. Jou, J. Casas-Vázquez, J. R. Madureira, A. R. Vasconcellos, and R. Luzzi, J. Chem. Phys. **116**, 1571 (2002).

[73] O. S. Duarte and A. O. Caldeira, Phys. Rev. Lett. **97**, 250601 (2006).